The Accuracy of Measuring Lumbar Vertebral Displacements Using a Dynamic MRI Sequence

A thesis presented to

the faculty of

the Russ College of Engineering and Technology of Ohio University

In partial fulfillment

of the requirements for the degree

Master of Science

Craig A. Goubeaux

May 2019

This thesis titled

The Accuracy of Measuring Lumbar Vertebral Displacements Using a Dynamic MRI Sequence

by

CRAIG A. GOUBEAUX

has been approved for

the Department of Chemical and Biomolecular Engineering

and the Russ College of Engineering and Technology by

John R. Cotton

Assistant Professor of Mechanical Engineering

Dennis Irwin

Dean, Russ College of Engineering and Technology

ABSTRACT

GOUBEAUX, CRAIG A., M.S., May 2019, Biomedical Engineering

The Accuracy of Measuring Lumbar Vertebral Displacements Using a Dynamic MRI Sequence

Director of Thesis: John R. Cotton

Lower back pain causes the second most doctor visits each year with over $100 billion spent annually. Excess motion of vertebrae due to lumbar instability is considered a main etiology of this pain. This study determines ex vivo accuracy and repeatability of a novel technique for measuring vertebral displacements by selecting corner points of each vertebra, on images captured using an Esoate G-Scan MRI, capable of upright, weight-bearing, dynamic imaging. The study was performed by moving a porcine lumbar vertebrae relative to another with known translational and rotational displacements. The translational measurements show high accuracy compared to the actual displacements (RMS error = 0.77 mm) and relative to the regression (SEE = 0.61 mm). The rotational measurements have increased errors compared to the actual displacements (RMS error = 4.23^0) and relative to the regression (SEE = 1.97^0). Both translational (average ICC(2,1) = 0.989) and rotational (average ICC(2,1) = 0.979) measurements show high degrees of repeatability. The technique developed may be used for future in vivo studies to further understand lumbar vertebral kinematics.

TABLE OF CONTENTS

Page

LIST OF TABLES

Page

LIST OF FIGURES

Page

CHAPTER 1: INTRODUCTION

Lower back pain, LBP, is one of the leading reasons for visiting the doctor. Treatment to alleviate this discomfort exceeds over $100 billion per year in the United States alone. The majority of these costs are attributed to loss in productivity or work missed due to elevated levels of pain (Lemonick et al., 2009). Excess motion of the vertebrae due to instability is believed to be one of the leading causes of LBP. It can be caused by a multitude of pathologies including tumors, spondylolisthesis, and intervertebral disc degeneration (Pope et al., 1992; Shin et al., 2013; Stokes and Frymoyer, 1987; Wang et al., 2008). In an effort to relate this motion to LBP, the relative displacements or kinematics of the lumbar vertebrae, specifically translation and rotation, have been studied by researchers. These measurements help to analyze vertebral motion during physiological conditions. With this data, researchers attempt to characterize instability, typically defined by abnormal movement of the vertebrae when an external force is applied (Hayes et al., 1989; White and Panjabi, 1978).

The data on the displacements of the vertebrae helps to answer questions such as what is normal and irregular vertebral motion, what is the etiology of the pain, and how to substantiate it (Li et al., 2009; Shin et al., 2013; Wang et al., 2008). To date, use of roentgenograms for static imaging or MRI combined with dual fluoroscopy for dynamic imaging, are the most common and effectively used techniques. They mainly analyze images of the lumbar vertebrae in the sagittal plane (Kozanek et al., 2009; Li et al., 2009; Passias et al., 2011; Shin et al., 2013; Teyhen et al., 2007; Wang et al., 2008; Xia et al., 2010). A drawback of these techniques is the exposure of patients to carcinogens from

the radiation used to develop the images. The American Cancer Society reports that cancer is the second leading cause of death in the United States, so avoiding the use of radiation-based methods could help prevent deaths due to cancer caused by radiation exposure (American Cancer Society, 2016).

Within the past 15 years a few studies have performed kinematic analysis using solely MRI such as McGregor et al. (2001) and Fujii et al. (2007). The use of MRI holds promise because by using a large magnet combined with radio frequencies to create images it is able to eliminate the use of harmful ionizing radiation experienced with roentgenograms or fluoroscopy. The images for these studies were taken in the supine position and different seated positions, respectively. These conditions neglect the physiological weight-bearing experienced while standing which provides the most accurate representation of the environment the vertebrae function within. More recently several studies have been published that have used upright-MRI to image individuals with LBP in different positions and collect different measurements (Nguyen et al., 2016; Rodriguez-Soto et al., 2013; Shymon et al., 2014; Splendiani et al., 2016; Tarantino et al., 2013). Although these studies did not quantify the relative displacements of the vertebrae, they were able to show that using upright-MRI to image differences in the anatomy of the lower back is effective. Also, limited studies have compared the kinematics of the vertebrae between asymptomatic and symptomatic patients with LBP, caused by lumbar instability, as did Passias et al. (2011). These previous studies have all successfully imaged and performed measurements of the lumbar vertebrae but have done so using different conditions and techniques.

In order to determine the accuracy of these measurements many studies such as Pearcy and Whittle (1982), Dvorak et al. (1990), and Teyhen et al. (2005) use cadaveric vertebrae to analyze the accuracy and repeatability of their techniques. The studies that have addressed this issue have found significant differences in the data. This can be contributed to changing variables such as image quality, examiners, experimental design, and techniques used to calculate the relative displacements (Cholewicki et al., 1991; Dvorak et al., 1991; Hayes et al., 1989; Pearcy and Whittle 1982; Pearson et al., 2011; Shaffer 1990; Teyhen et al., 2005; Yeager et al., 2014). These studies also state the difficulty in comparing the accuracy of studies due to the different statistical measurements reported. All of these factors contribute to the discrepancies of the *gold standard* technique appropriate for imaging and measuring the relative displacements of the lumbar vertebrae, validating the technique's accuracy, and then using the data to quantify instability to relate it to pain in symptomatic patients.

1.1 Specific Aims

This study used the Esaote G-Scan Brio 0.25-Tesla MRI to take multiple images of two-segment porcine lumbar spines adjusted into various positions. The relative positions were measured both physically on an apparatus and from the MR images and tested for their accuracy and repeatability.

(1) I designed and fabricated an apparatus that holds a two-segment lumbar pig specimen capable of moving the top vertebra with five degrees of freedom relative to the bottom vertebra.

(2) Vertebral segments from two pigs were placed at 8 randomly selected rotations and translations each. This was done for lateral bending (frontal view) and flexion-extension (lateral view). Two different MRI sequences were used and compared for each: T1 and 2D HYCE S.

(3) The relative positions were measured using a manual method I developed in Matlab. These positions were compared to the physical measurements from the apparatus. The accuracy and repeatability of the manual method was calculated.

This experiment is the first of its kind. The information will quantify the accuracy and reliability of the use of a 0.25-Tesla upright-MRI capable of taking dynamic images in conducting vertebral measurements. This will establish a safe alternative to commonly used ionizing imaging techniques, such as CT and DFV, for accurately measuring the relative displacements of the spine.

CHAPTER 2: LITERATURE REVIEW

2.1 Lumbar Spine Anatomy

In the human body there are five lumbar vertebrae located at the base of the midline of the back labeled L1-L5, superiorly to inferiorly (Figure 1). Each individual vertebra is comprised of an oval-shaped vertebral body from which two pedicles protrude from the posterior aspect. These then connect to two laminae and seven processes. The posterior portion of the vertebral body, the pedicles, the laminae, and processes form the vertebral foramen. This structure forms the spinal canal which is the pathway through which the spinal cord passes. The superior articular processes of an inferior vertebra interact with the inferior articular processes of the adjacent superior vertebra to form the facet joints. These joints help to maintain the stability of the spine by reducing excess motion. In between each adjacent vertebral body there are intervertebral discs, oval-shaped segments of fibrous cartilage between each spinal vertebra that give support and flexibility to the spine. In addition to the facet joints and intervertebral discs, the muscles and ligaments connected to the processes largely affect the movement and stability of the vertebrae. These physiological characteristics affecting the stability of the spine add variables that increase the complexity of measuring the movements of the lumbar vertebrae.

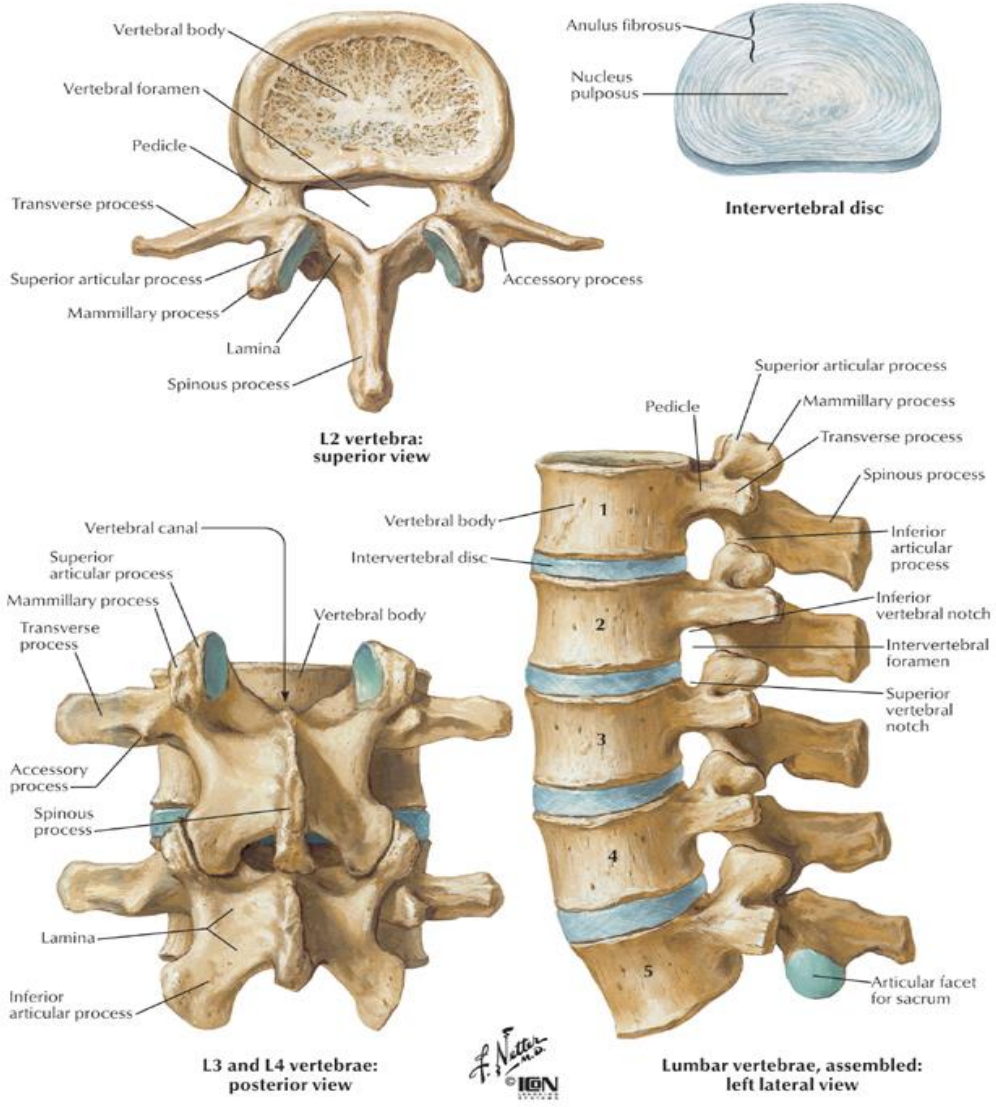

Figure 1: Top Left – Superior view of individual vertebra. Top Right – Superior view of individual intervertebral disc. Bottom Left - Two-segment posterior view. Bottom Right – Lateral view of lumbar spine labeled 1-5. (Cochard et al., 2012)

Further increasing the difficulty of studying the lumbar spine during physiological movements, such as flexion-extension or lateral bending, are the coupled motions of the vertebrae. With any desired translation or rotation there is an additional passive movement which accompanies. For example, in lateral bending the vertebrae translate

and rotate in the coronal plane, but they also axially rotate in the transverse plane therefore causing a coupled motion (Figure 2) (White and Panjabi, 1978).

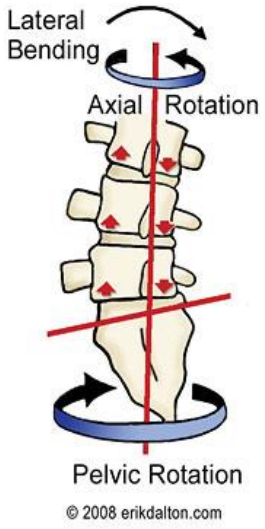

Figure 2: A lumbar spine performing lateral bending movement in the coronal plane, accompanied by an axial rotation in the transverse plane (Dalton, 2008).

2.2 Lower Back Pain and Instability

LBP is the second leading cause for trips to the doctor with 60-90% of adults experiencing it in their lifetime (Lemonick, 2009). Shaffer et al. (1990) states that 80-90% of patients with LBP are unaware of the origin or reason for their pain, with the other 10-20% having a visible anatomical pathology explaining their symptoms. Lumbar vertebrae are known to work together as a functional unit to provide the flexibility necessary for individuals to perform specific tasks. The collection of the vertebrae, muscles, and ligaments maintain the integrity of the spine and work to keep the vertebrae within their normal range of motion. When the integrity of the spine is compromised

leading to abnormal vertebral movement, the spine becomes unstable. This instability is thought to be the pathology most associated with LBP (Shin et al., 2013).

Hayes et al. (1989) reports that The American Academy of Orthopaedic Surgeons defined segmental instability as, “an abnormal response to applied loads characterized by motion in the motor segment beyond normal constraints” (p. 327). White and Panjabi (1990) expand upon this definition and incorporate the clinical aspect of instability by defining it as, “the loss of the ability of the spine under physiologic loads to maintain its pattern of displacement so that there is no initial or additional neurological deficit, no major deformity, and no incapacitating pain” (p. 278). These are two well-structured definitions of instability but in both cases they hinge on the fact of knowing what constitutes normal motion in an asymptomatic spine and comparing that to the motion of an unstable, pathological spine. Fujii et al. (2007) supports this by claiming that before it can be clinically diagnosed that a spine is unstable and therefore pathological, there has to be a set standard as to the normal kinematics of the vertebrae.

Quantifying the normal, asymptomatic kinematics of the lumbar vertebrae provides a baseline for comparison to a symptomatic patient with LBP to successfully diagnose lumbar instability. Many recent studies on the lower back aim to measure the displacements of the vertebrae relative to one another in asymptomatic patients (Fujii et al., 2007; Hayes et al., 1989; Li et al., 2009; Shin et al., 2013; Xia et al., 2010). Currently, there is disagreement on the accepted diagnosis of lumbar instability. Typically, the standard quantity used is a translation of greater than 4 mm of one vertebra relative to another (Pearson et al., 2011). However, Yeager et al. (2014) reports multiple

different values ranging from 3 to 4.5 mm of translation and 10 to 25 degrees of intervertebral rotation (IVR). There has been much debate about these measurements leading to the lack of a widely accepted *gold standard* criteria for the diagnosis of instability. There is still large disagreement as to what defines normal vertebral motion and additionally how to quantify motion that exceeds these limits and is clinically important (Muggleton and Allen, 1998). Numerous reasons cause the skepticism of this rule, among them: the inability to quantify the normal kinematics of the lumbar vertebrae, the broad range of values reported for translations and rotations of vertebrae in asymptomatic patients, the varied methods used to image the vertebrae and calculate their relative displacements, and the inability to quantify what translation or rotation of vertebrae relative to one another induces pain in a patient.

The lack of knowledge and consensus on the normal kinematics of the lumbar vertebrae and the kinematics appropriate for diagnosis of a symptomatic patient with instability has far reaching affects. Having a firm understanding of the kinematics of the lumbar vertebrae will improve upon the clinicians' intellect of specific pathologies and their etiologies. As a result, the misdiagnosis of LBP due to instability will decrease leading to improved decision making on appropriate treatments and procedures.

In the realm of lumbar instability, decreased misdiagnosis and improved decision making on treatments and procedures would help solve the problem of the drastic increase in cases of lumbar fusions. Many of these are performed because of wrongful diagnoses of patients with LBP thought to have instability. These errors occur because of the lack of sufficient techniques used to image and measure the kinematics of lumbar

vertebrae. It is then difficult to equate those findings to instability resulting in LBP. Many times instability is confused with hypermobility. This may or may not cause pain depending on the properties of the ligaments and muscles interacting with the vertebrae (Muggleton et al., 2000). Fusions are commonly used to correct instability and are performed between two adjacent vertebrae where pain is present. This is done in an effort to stabilize the vertebrae to relieve the pain. This joining of the vertebrae results in modified vertebral motion (Li et al., 2009). Therefore, when fusions are performed unnecessarily the probability increases that additional pathologies will develop (Figure 3). Additionally, the procedure is expensive, painful, and has a high amount of risk. By further understanding the vertebral kinematics, clinicians would be able to better diagnose patients and decide on those who would benefit from spinal fusions to correct instability (Li et al., 2009). Also, back surgery success rates would increase and medical costs would decrease as a result of addressing the correct pathology (Teyhen et al., 2005).

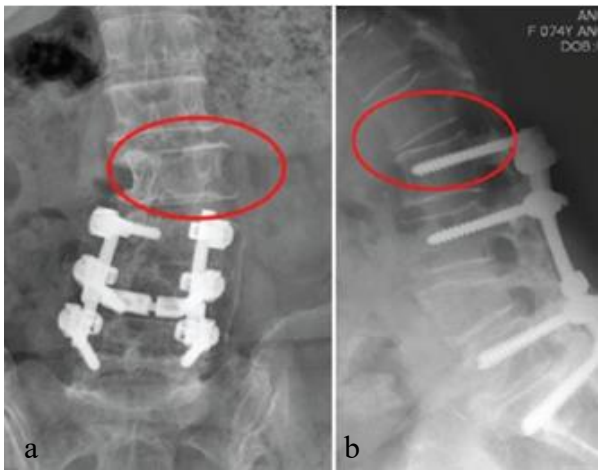

Figure 3: Lumbar fusions: (a) Posterior view of a lumbar segment showing pathology by excess translation adjacent to a lumbar fusion, (b) Lateral view of a lumbar segment showing pathology by excess rotation adjacent to a lumbar fusion (Ha et al., 2013).

2.3 Imaging Techniques of the Spine

The imaging methodologies used to study the kinematics of the lumbar vertebrae have advanced greatly over the years. Imaging of the spine began as far back as 1928 by the use of roentgenograms. Further advances were made in the early 1980's when calibrated X-ray images and videofluoroscopy began widespread use. Today, MRI with dual-fluoroscopy is the main imaging technique. As the technology has advanced, so has the quality of images obtained and the amount of information gathered. Each technique has advantages and disadvantages associated with it including image quality, radiation exposure, cost of use, and sequence parameters. Therefore, the aims of each study must be clearly defined in order to decide upon which method to use, in addition to the use of one that is at the disposal of the researcher.

Todd and Pile in 1928 along with Bakke in 1931 were the first researchers to use x-rays to acquire roentgenograms of the spinal anatomy of humans for measurements (Bifulco et al. 2001). Figure 4 shows the lack of quality of roentgenograms at that time. In 1944 and 1953, Gianturco and Tanz respectively, began to improve upon the techniques set forth by Todd and Pile and Bakke by calculating the angles between respective vertebrae of the spine at end range-of-motions in symptomatic and asymptomatic patients with LBP (Bifulco et al., 2001). This laid the groundwork for the next 70 years.

Figure 4: Posterior, coronal view of a roentgenogram of the lumbar spine (Tanz, 1953).

The use of roentgenograms as a means to image the lumbar vertebrae was utilized by researchers such as Hanley et al. (1976), Dimnet et al. (1978), Taylor and Twomey (1980), Shaffer et al. (1990), and Dvorak et al. (1991). In the infancy of its use the images were grainy and difficult to analyze providing varied data and inconsistent conclusions. Also, the images acquired were only in two-dimensions, when in vivo the spine moves in three-dimensions. This prompted the development of a new technique using a biplanar radiography system developed at Oxford that captured images in two different planes (Figure 5) (Stokes et al., 1981).

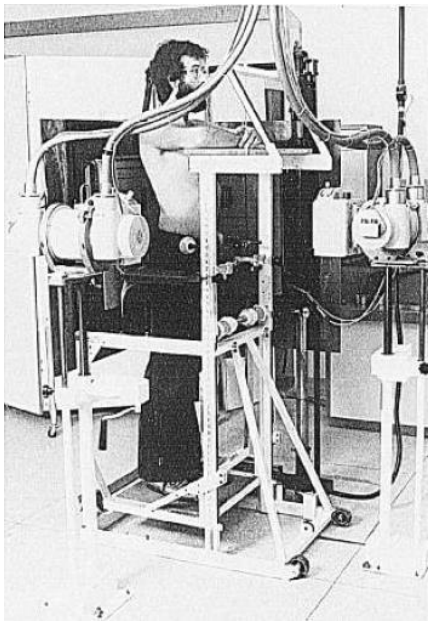

Figure 5: Scanning of a subject using biplanar radiography (Pearcy et al., 1985).

By using two radiographs, one capturing the sagittal plane and the second the coronal plane, two differently oriented images in various static phases are acquired. Nine identical anatomical landmarks are then selected on each vertebra of each image. These landmarks are then calibrated and a three-dimensional coordinate system assigned. Through a direct linear transformation technique, the three-dimensional coordinates of each point can be obtained at the different static positions imaged. The relative translations and rotations of the vertebrae can then be calculated by identifying four landmarks from the previous nine selected (Pearcy and Whittle, 1982). This marked the first time three-dimensional analysis of the lumbar vertebrae had been accomplished which put in motion the technology for future researchers such as Pearcy et al. (1984 & 1985), Cholewicki et al. (1991), and Panjabi et al. (1992). This development not only helped analyze the movement of the lumbar spine in three-dimensions, but also helped

research on many other anatomical features such as the hip (Moreside et al., 2013), the pelvis (Mahaudens et al., 2005), and the thoracic and cervical spine (Fiebert et al., 1993).

The use of biplanar radiography was a huge advancement in imaging technology but a drawback of this technique was the ability to only capture static images. Further improvements were made in medical imaging through the development of a real-time image acquisition technique. This new technique took active x-ray images in either the sagittal or coronal plane and recorded them through a television camera within an image intensifier (Figure 6) (Breen et al., 1988 & 1989).

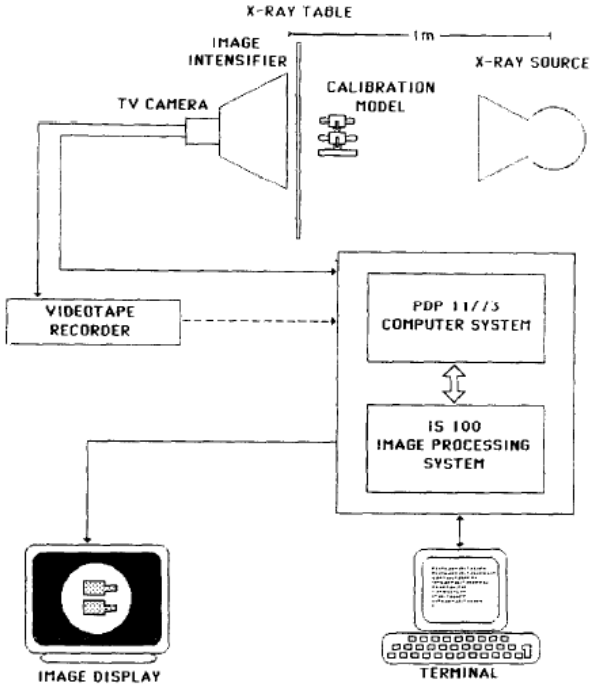

Figure 6: Diagram of real-time imaging system (Breen et al., 1988).

This development provided the ability to analyze patients throughout physiological movements rather than static positions at the end of a movement. Also, this provided a more detailed representation of how the vertebrae move in vivo based on

factors such as upper-body weight, ligament and muscle activation, and dynamic, voluntary motion (Fujii et al., 2007; Lee et al., 2002; Muggleton et al., 2000; Teyhen et al., 2005). This method of image acquisition has been utilized by many researchers in the field of spinal analysis such as Cholewicki et al. (1991), Page and Monteith (1992), Van Mameren et al. (1990), Kanayama et al. (1996), Okawa et al. (1998), and Teyhen et al. (2005). Although it was now possible to visualize the vertebrae actively moving, this new technique sacrificed the ability to analyze the vertebrae in three-dimensions.

Further, advancements were made in image acquisition by use of Digital Fluoroscopic Videos (DVF) combined with MRI. This technique was essentially a combination of the work done by Pearcy and Whittle (1982) and Breen et al. (1988) described previously with the additional use of a static MR image. Initially, patients are scanned using MRI in the supine position to acquire stacks of images in order to create computer generated three-dimensional models of the vertebrae. Then the patients are situated in a standing position between two orthogonally placed x-ray sources and asked to perform specified movements to capture real-time videos via the dual fluoroscope. The previously developed 3-D models are then calibrated to the video acquired through dual fluoroscopy and move accordingly (Li et al., 2009; Shin et al., 2013; Wang et al., 2008; Xia et al., 2010). With this technology, it is possible to calculate the three-dimensional coordinates of the vertebrae throughout a movement. Also, it is possible to create real-time videos of model spines of patients performing varied movements. This allows for visualization of the vertebrae in three-dimensions under active, physiological weight-bearing conditions for a more realistic representation of how the vertebrae move

dynamically. This ability to analyze kinematic data of the vertebrae in all three dimensions has led to further understanding of rotations and coupling motions of the vertebrae during specified movements.

The use of DVF in combination with MRI is a great technique for analyzing vertebrae under physiological, weight-bearing conditions. Despite its advantages, this technique exposes the patients to potentially harmful radiation because of the x-rays that pass through the patients' bodies. Bifulco et al. (2001) reports that the average radiation exposure from a radiograph of the lumbar spine is about 20 mGy (milligray) for an anterior-posterior view and 50 mGy for a lateral view. These values are then multiplied by a tissue weighting factor (0-1) for each organ in the body based on the effects radiation has on it. This gives a value measured in milliSieverts (mSv). According to the Health Physics Society, an individual should not be exposed to more than 50 mSv a year and 100 mSv in a lifetime. Exceeding these dosages has been shown to increase the likelihood of cancer. Yet, remaining below these doses has not been proven to prevent disease. Therefore, a patient could be exposed to more or less radiation depending on the duration of imaging. These images are taken of the midsection of the body which exposes many vital organs to this harmful radiation. The use of MRI eliminates any need to expose bodily organs to radiation.

Limited studies have utilized solely MRI to analyze the kinematics of the spine. A major limitation of the MRI machines used by Fujii et al. (2007) and McGregor et al. (2001) is that they are unable to perform any active movements or weight-bearing conditions while acquiring the images of the vertebrae. The future of understanding the

normal and eventually the pathological displacements of the spine is in accurate and reliable comparisons of symptomatic and asymptomatic patients with LBP due to lumbar instability. But this should not be done at the expense of exposing patients to carcinogens as DVF does. Therefore, it is important that research on LBP caused by instability move towards the sole use of MRI and developing a way to do so in functional, weight-bearing conditions.

2.4 How MRI Works

MRI is an imaging technique that is noninvasive and does not exposure a patient to harmful ionizing radiation. It has been described as one of the most flexible medical imaging techniques in the field of medicine (Modic et al., 1989). MRI is based on hydrogen atoms located in bodily tissue and fat, which are found mostly in water. Hydrogen atoms all have a specifically oriented spin. The MRI consists of a large magnet that produces a magnetic field. When hydrogen atoms are placed in this field they will align either north or south because of their polarity. The atoms oriented in opposing directions will cancel out leaving a collection of atoms oriented in one direction that do not have a partner to cancel out. A radio frequency is then applied to these atoms causing them to spin in the opposite direction. Once the radio frequency is turned off, they return to their original position releasing energy. Each type of tissue will release differing amounts of energy and therefore different waveforms. These waveforms are received by the coil surrounding the body part being imaged. Through the process of Fourier transform each waveform is categorized by the sum of its sinusoids (Bevel, 2010). The MRI is then able to create a grayscale image from the tissue classifications

based on their waveforms. This process can be done for any desired section of the body for any number of slices (Gould, 2008; Modic et al., 1989). The fact that MRI doesn't exposure the patient to ionizing radiation makes MRI one of the safest imaging techniques available.

2.5 Techniques for Calculating Relative Positions of the Spine

Along with imaging technique, the types of calculations used for kinematic analysis of the movements of the vertebrae are equally important. White and Panjabi (1978) borrow an analogy from Lovett (1905) that compares the vertebrae to the cars of a train. They propose questions such as: "What alterations of the train will change the course it takes, the distance it travels, or the smoothness of the ride?" and "How far outside its usual course can it travel without being in danger of malfunctioning?" This analogy may see elementary when describing the kinematics of the spine but in reality it holds valid comparisons. A train must travel on a specified path in a particular manner to function optimally and so too must the spine. There are many different ways to calculate the displacements of the lumbar vertebrae relative to one another, but this has led to increased difficulty in comparing the results of different studies. This is evident when there are different assumptions in the setup of a study, such as the comparison between Breen et al. (1989) and Cholewicki et al. (1991), where different displacements are used for determining the accuracy of their measurement technique. Also when different measuring techniques are used, like those in Frobin et al. (1996) compared to Hanley et al. (1975), where Frobin et al. (1996) employs a much more detailed process. This has led to variability in the data that has been reported (Muggleton and Allen, 1998). Similar

to standardizing the normal movements of the vertebrae, establishing a standardized set of calculations to analyze relative vertebral displacements and determining its accuracy would aid in the comparison of results from different studies.

In the mid 1970's, research was prevalent on the relative displacements of the cervical and thoracic spine but little progress had been made on the lumbar spine. Furthermore, research that was being done was only measuring rotations of relative vertebrae while neglecting to analyze their relative translations (White and Panjabi, 1978). Researchers such as Wiles (1935) and Allbrook (1957) were some of the first to study the full range of motion of the lumbar spine. This helped with understanding the overall movement of the spine, but didn't pinpoint the root cause of LBP due to instability. Tanz (1953) was one of the first to calculate relative rotations between vertebrae. One of the first methods employed by early researchers (Begg and Falconer, 1949; Froning and Frohman, 1968; Tanz, 1953; Wiles, 1935) for calculating angles of flexion and extension in the lumbar spine was to draw a line on the superior or inferior endplate of a vertebra. Then, superimpose another image, at a different position, over top of the previous image and draw an identical line on the same vertebra. These lines would then be extended until they intersected and a protractor would be used to measure their angle. Tanz (1953) reported an error of 2^{o} when performing this technique a second time on the same images. This was in agreement with the findings of Froning and Frohman (1968). Hanley et al. (1976) then improved upon this method by adding lines drawn from the antero-superior to the postero-inferior corner of each vertebra. Additionally, they added lines drawn on the superior and anterior endplates of the sacrum to align the

superimposed images (Figure 7). This procedure was performed twice, blinded to the original results. The comparison of their measurements was within 1° or less. Variations of this hand-tracing method continued to be used by researchers such as Dvorak et al. (1991) and Panjabi et al. (1992). It was compared to computer automated methods and no significant difference between the measurements was found, with the largest difference being 1.9° for lateral bending. This seemed to show good reliability of the method but it still lacked sufficient accuracy.

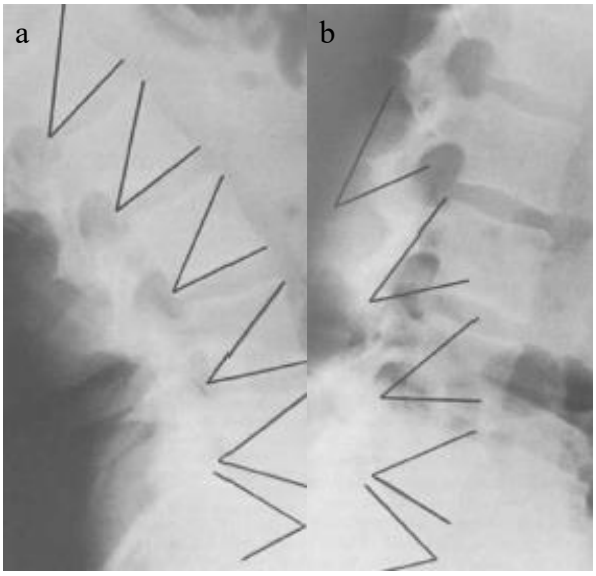

Figure 7: Kinematic measurement technique: (a) Roentgenogram in sagittal plane in flexed position, (b) Roentgenogram in sagittal plane in extended position (Hanley et al., 1976).

In the early 80's, a new technique began to be commonly used. Taylor and Twomey (1980) measured the angles of the lumbar spine during flexion-extension using a lumbar spondylometer and during axial rotation using a lumbar rotameter (Figure 8). This gave data on the rotations of the spine as-a-whole, not relative vertebral rotations.

They reported that this technique underestimated the actual range of motion by 1°. The largest variance when a second observer performed the measurement was 5°, possibly indicating poor repeatability or other operator dependent errors. Their data was compared to a study done by Twomey (1979) that used cadaveric spines. This study also found a wide variance between the first and second observer performing the same procedure. Studies such as Fracs and Harris (1983) and Pearcy and Hindle (1989) tried similar techniques and reported similar errors. Few studies have since used these techniques because of the difficulty in measuring vertebral motion on the surface of the skin with the interference of tissue.

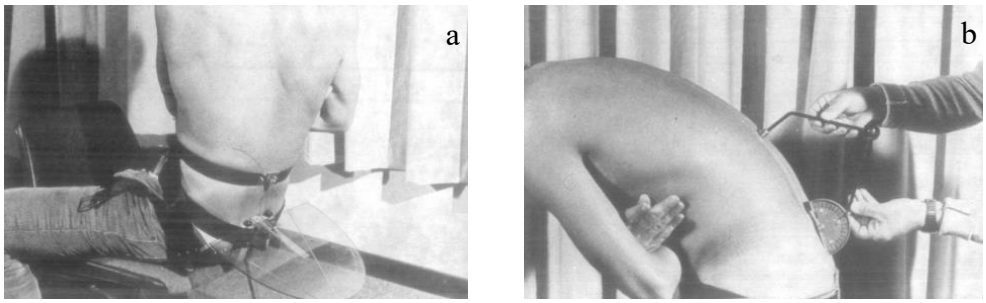

Figure 8: Kinematic measurement technique: (a) Flexion measurement by use of a lumbar spondylometer, (b) Axial rotation measurement by use of a lumbar rotameter (Taylor and Twomey, 1980).

Following the unsuccessful attempts of the surface procedures, many researchers turned to the use of biplanar radiography to measure the relative displacements of the lumbar vertebrae. Pearcy and Whittle (1982) were one of the first to develop a digital technique for three-dimensional analysis. The three-dimensional, relative displacements of each vertebra were able to be measured through a process of acquiring orthogonal images, selecting nine similar anatomical landmarks on each vertebra in each two-

dimensional image (Figure 9), digitizing the coordinates of each landmark, and using a direct linear transformation technique that related the two-dimensional landmarks of each image into three-dimensions. The coordinates could then be tracked through the series of images in order to provide more detailed measurements of the kinematics of the vertebrae. This technique was performed selecting nine anatomical landmarks and also four. Overall the RMS errors stayed below 2 mm for translation and 1.5º for rotation. However, when selecting four landmarks as opposed to nine the errors increased, almost doubling in some cases. This demonstrates the effect increased points have on reducing the error in measurements. This technique was utilized by many researchers such as Pearcy et al. (1984 & 1985) and Stokes and Frymoyer (1987). This development furthered the knowledge of vertebral movement, but was only capable of analyzing static, end range-of-motion images.

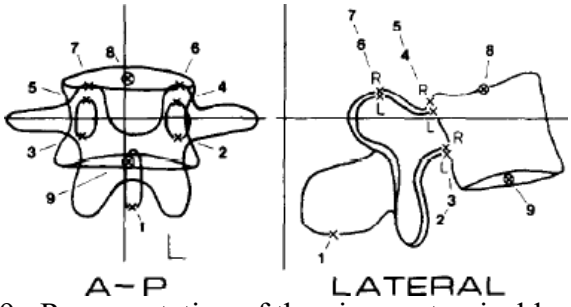

Figure 9: Representation of the nine anatomical landmarks chosen on each vertebra (Pearcy and Whittle, 1982).

Imaging the complete range-of-motion of the vertebrae was first done by Breen et al. (1988) using the real-time imaging technique described previously. Measuring the relative vertebral displacements from this was done on the digitized images of one subject by selecting two corner points, either the two anterior for sagittal views or the two

inferior for coronal views, and calculating the angle from the vertical or horizontal, respectively. Cholewicki et al. (1991) improved upon this method by selecting the four corner points of each vertebra and digitizing each four times to reduce error. Breen et al. (1988 &1989) reported mean absolute errors of 0.56±0.37º for the coronal plane and 0.84±0.87º for the sagittal plane, compared to Cholewicki et al. (1991) that reported errors of 0.465±0.288º for rotation overall after optical distortions had been corrected. Cholewicki et al. (1991) stated that the error more than doubled when the image was distorted even after the digitization process, suggesting image quality as an important factor in calculations. Further improvements were made by Bifulco et al. (2001) where they selected the four corner points of each vertebra on the first image. These four points were then selected on the subsequent images using a template generated through automatic landmark recognition by cross-correlation in order to eliminate the error associated with manually picking the points (Figure 10). All relative rotations calculated by this method were within 1º of the actual angle and their standard deviations never exceeded 0.3º, indicating good repeatability.

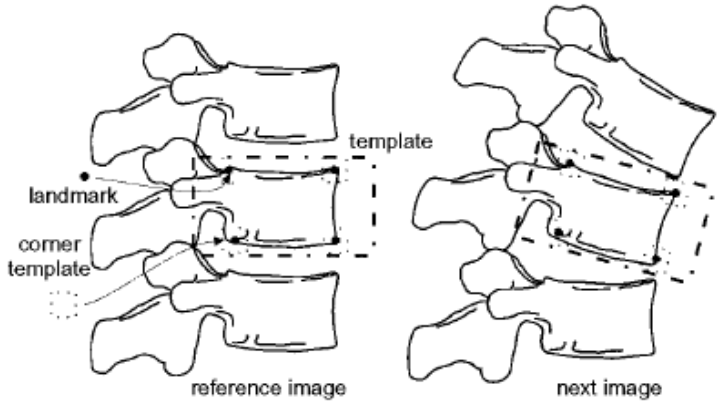

Figure 10: Representation of template generated and superimposed on subsequent images (Bifulco et al., 2001).

Due to the large influence of image distortion on kinematic calculations, Frobin et al. (1996) presented a new measurement technique not affected by distortions due to central projection, axial rotation, lateral tilt, and off-center position (Figure 11). This technique selects the four corner points on a sagittal image, two anterior and two posterior. Then two midpoints are selected, one between the two anterior corner points and one between the two posterior corner points. Additionally, an overall midpoint of the vertebral body is selected between the anterior and posterior midpoints. A midplane is then formed by connecting these three midpoints. The angle between adjacent midplanes is used to measure the rotation of the vertebrae throughout movements. Their differences are compared at different positions to measure their relative rotations. Calculating translations is done by forming the bisetrix, a line drawn equally between the two midplane lines. A perpendicular line is drawn from the overall midpoint of each vertebra that intersects with the bisetrix. The distance between the intersection points of the two perpendicular lines is divided by the mean depth of the superior vertebra to get the translation. This is done to standardize the measurement in regards to magnification and

patient differences. The errors reported for this technique range from 0.7-1.6° for rotation and 0.4-0.8 mm for translation, with error increasing at more inferior segments (i.e. L4-L5 has more error associated with its measurement than L1-L2).

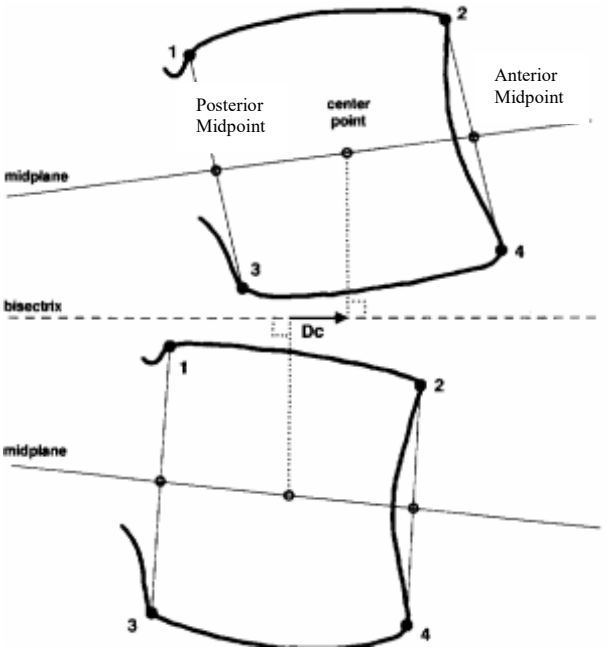

Figure 11: Schematic showing kinematic measurement technique developed by Frobin et al. (1996).

These measurements use point selection of specific anatomical landmarks to create lines. This avoids the use of tangent lines to outline the vertebral body, as were used in Harvey and Hukins (1998). These methods have been shown to cause increased error because of the convex nature of vertebral bodies whereas specific landmarks reduce this error (Frobin et al., 1996). Panjabi et al. (1992) found that lines drawn on the anterior and posterior surfaces of the vertebral bodies in the sagittal view had significant error, while those drawn on the superior and inferior endplates had much less. However, the method used by Harvey and Hukins (1998) proved that the calculated center points on

the vertebral bodies was not influenced by variation in point placement. They concluded that the path of the center points is the best measurement of vertebral kinematics. Teyhen et al. (2005) improved the accuracy of the measurements of this method by using a process of four different enhancement techniques to improve the clarity of the radiographs. Then the vertebral corner and midpoints were selected as described previously by Frobin et al. (1996). These points were digitized four times as was done by Cholewicki et al. (1991) in order to minimize error. After calculating the relative displacements of the vertebrae, they reported at individual vertebral levels errors half of those reported by Frobin et al. (1991) and in some cases even less.

Within the last decade measuring vertebral kinematics has moved towards generating three-dimensional models of the vertebrae and analyzing their movement. The vertebrae are created through a process of segmentation of MR images. They are then registered to every image captured by dual-fluoroscopy throughout the movement being studied (Figure 12). A three-dimensional coordinate system is then assigned to the images and the relative displacements can be calculated accordingly (Fujii et al., 2007; Li et al., 2009; Shin et al., 2013; Xia et al., 2010). Fujii et al. (2007) reported errors of 0.24° for flexion-extension, 0.31° for lateral bending, 0.43° for axial rotation, 0.52 mm for superoinferior translation, 0.51 mm for anteroposterior translation, and 0.41 mm for lateral translation for their methods. Li et al. (2009), Xia et al. (2010), and Shin et al. (2013) simply reported data on the displacements of the vertebrae, failing to report the accuracy or repeatability of their procedure.

Figure 12: Segmented 3-D models of lumbar vertebrae registered to the two images captured by dual-fluoroscopy (Xia et al., 2010).

It is evident that many techniques have been developed and implemented throughout the history of studying the lumbar spine and measuring its relative displacements. Yet there still has not been agreement on what technique provides the best results and should be regarded as the *gold standard* (Muggleton and Allen, 1998). Throughout the review by Muggleton and Allen (1998) they discuss numerous methods used to measure translation, either in regards to a fixed or moving reference frame, and discuss how it adds ambiguity to the comparison of different studies. Also, many studies have been done to investigate the accuracy and repeatability of manual vs. automated methods for calculating vertebral kinematics. Pearson et al. (2011) reported a median absolute difference of 1.3^{o} for rotation and less than 1 mm for translation between a Quantitative Motion Analysis (QMA) technique and a digitized manual technique. However, the standard errors of measurement (SEM) of rotation were 2.5^{o} for the manual technique compared to 0.5^{o} for the QMA technique. Additionally, the SEM of translation was 2.3-2.8 mm for the manual technique compared to 0.3-0.6 mm for the QMA technique. Intraobsever and Interobserver reliability were both reported as being *substantially higher* for the QMA technique compared to manual. Yeager et al. (2014)

supports these findings through a similar study comparing a new Vertebral Motion Analysis (VMA) system to a digitized manual technique. Overall, the numerous ways to calculate the vertebral kinematics causes difficulty in comparing studies. By implementing a standard measurement technique, different studies would be more relatable and increase the knowledge of the relative displacements of the lumbar vertebrae.

2.6 Techniques for Determining Accuracy of Measuring Relative Displacements

Measuring the relative displacements of the lumbar spine helps clinicians understand how the vertebrae are moving in order to quantify different pathologies which aids in the diagnosis and treatment of LBP. The movements of the vertebrae relative to one another during specific movements occur in incrementally small measurements (translations measured in millimeters and rotations measured in degrees). Therefore, high accuracy and repeatability of these measurements is desired because small errors will lead to incorrect measurements and inappropriate diagnoses of instability causing LBP. To validate the accuracy of the data reported from a specific method different statistics can be reported.

One statistical calculation is to perform measurements on each image multiple times and report the standard deviations. This provides the variance in a method like Kanayama et al. (1996) which reported standard deviations between 0.5-0.7 mm for translation and 1.0^{o} for rotation. Many other studies have used cadaveric vertebral models to validate the accuracy of their method for in vivo use (Figure 13) (Bifulco et al., 2001; Breen et al., 1988 & 1989; Cholewicki et al., 1991; Frobin et al., 1996; Hanley et

al., 1976; Ishii et al., 2004; Pearcy and Whittle, 1982; Shaffer et al., 1990; Stokes et al., 1981; Taylor and Twomey, 1980; Wang et al., 2008). These studies orient the vertebral specimen in known translations and rotations. Then they perform their measurement technique and compare its results to the known orientations. This provides a good analysis of the accuracy of the method used.

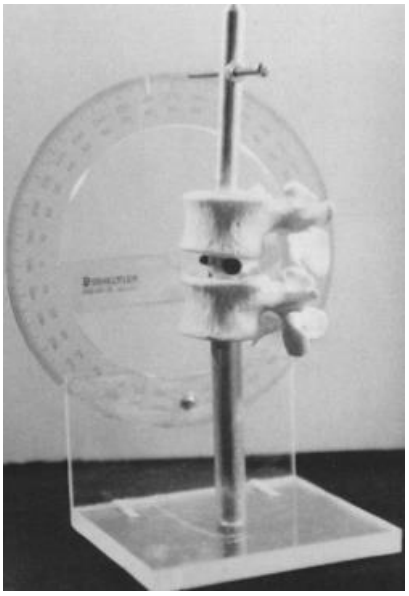

Figure 13: Example setup of testing the accuracy of a measurement technique using a cadaveric model (Cholewicki et al., 1991).

The difficulty in comparing these different studies is they do not all use the same predetermined orientations, experimental design, and statistical tests to validate the accuracy of the techniques. Taylor and Twomey (1980) used a spondylometer to measure the full range-of-motion of the lumbar spine on the surface of a patient's skin. To test the accuracy of this method, a force was applied to cadaveric specimen through an apparatus that mimicked the full range-of-motion in vivo of the lumbar spine in the

sagittal plane. The rotational measurements of the spine were then taken by the spondylometer and a protractor and compared. The spondylometer was found to routinely underestimate the actual relative angle of the vertebrae by 1.0±1.0°. This validation technique differed from many of the other studies because of their use of surface measurements and the application of a force on the cadaveric vertebrae.

To test the accuracy of the technique used by Pearcy and Whittle (1982) for selecting anatomical landmarks only five unspecified movements were performed that were measured three times each providing 15 measurements. It was found to have RMS errors ranging from 0.17-2.07 mm for translation and 0.69-1.36° for rotation. Breen et al. (1988) performed a more elaborate study rotating the superior vertebra in the sagittal and coronal plane in 2° increments through 20° relative to the inferior vertebrae. Two additional trials were performed with the entire specimen rotated 10° orthogonally and 10° inferior to the main X-ray source. The mean differences ranged from 0.30° to 0.84° with standard deviations ranging from 0.18° to 0.45°. Breen et al. (1989) later tested the accuracy of their method by rotating the superior vertebra relative to the inferior in 5° increments through 30° of rotation in the coronal plane. Also, the superior vertebra was axially rotated 1° for every 2° of rotation in the coronal plane. Before imaging, 10 cm of animal tissue was placed between the X-ray source and the specimen to simulate in vivo imaging. The mean difference was 0.5±0.37°. Variations of these techniques have been the most widely used.

A slightly different method was Cholewicki et al. (1991) where the superior vertebra was rotated 0°, 5°, and 10° in the sagittal plane relative to the inferior vertebra.

A plastic jar filled with water was situated between the X-ray source and the specimen in order to simulate the in vivo environment as Breen et al. (1989) did with animal tissue. The error found in this method was 0.44±0.43 mm in translation and 0.870±0.842° in rotation for the uncorrected optical distortions, but was 0.22±0.17 mm and 0.465±0.288° once corrected. Frobin et al. (1996) similarly rotated the superior vertebra relative to the inferior vertebra in the sagittal and coronal planes but for -5°, 0°, and 5° orientations. The standard deviations reported for this method ranged from 0.4-0.8 mm for translation and 0.74-1.64° for rotation at different levels of the spine. Bifulco et al. (2001) again rotated the superior vertebra relative to the inferior vertebra in 5° increments through 20° of rotation in the sagittal and coronal plane. The mean errors were reported as less than 1° with no greater than 0.3° standard deviation. These studies all rotated the superior vertebra relative to the inferior vertebra in either the sagittal plane, coronal plane, or both. The specimens were all positioned in differing degrees of rotation with diverse parameters in order to calculate the statistical accuracy of their method. However, it is difficult to find two studies that have performed the same procedure complicating the comparison of different measuring techniques.

This difficulty is evident in the study published by Teyhen et al. (2005) attempting to compare their SEMs of 0.40° to 0.72° to the findings of Frobin et al. (1996). Teyhen et al. (2005) is unable to definitively state that their method is more accurate than Frobin et al. (1996) because of the differences in their design and statistical analyses performed. Some studies such as Hanley et al. (1975), Stokes et al. (1981), and Ishii et al. (2004) don't even report the statistical tests used to calculate the accuracy of their

methods, they simply state that the accuracy was tested. Also, the previously discussed studies all tested their accuracy on rotations neglecting translations. A study done by Pearson et al. (2011) found that for both manual and automatic measurements of relative displacements, rotations were more accurate than translations. This may explain the reason why studies fail to test or report the accuracy of their measurement method for translations. One possibility could be a millimeter (unit used for measuring translation) is a smaller incremental measurement than a degree (unit used for measuring rotation). All of these differences and uncertainties in a standardized approach for statistical verification have led to the inability to definitively compare the accuracy of different studies.

An additional statistical test is intra- and interobserver comparisons. The benefit of performing these tests is the determination of the repeatability of the method. Intraobserver is the comparison of the same individual performing the same task at different points in time, while interoberserver is the comparison of different individuals performing the same task. Fewer studies have performed these tests in order to validate the repeatability of their method (Dvorak et al., 1990; McGregor, 2001; Pearson et al., 2011; Shaffer et al., 1990; Yeager et al., 2014). Dvorak et al. (1990) used two observers and found that their intraobserver differences were 1.6º for flexion-extension and 2.5º for lateral bending. For the interobserver differences the two observers measured one radiograph six times at four segmental levels which provided a standard deviation of 1.25º. Shaffer et al. (1990) compared the translation measurements of two observers using three different measurement methods on 58 flexion-extension roentgenograms. For

flexion-extension films the intraobserver correlations varied from 0.604 to 0.909 for the two observers over all three methods. The interobserver correlations varied from 0.359 to 0.836. These wide variances should be further evaluated to see if certain measurement techniques need to be excluded or refined.

Additional studies such as Pearson et al. (2011) used three orthopaedic surgery residents as their observers for their study. Yeager et al. (2014) similarly used three physicians (Table 1). Intraclass correlation coefficients (ICC) were used to compare observer measurements in both studies (0 being no agreement and 1 being complete agreement). These numbers indicate that rotations are more reliable than translations when measured within and between observers. The fact that these studies performed similar statistical tests provides easy comparison in their results. Trying to compare these correlation coefficients to other studies such as Dvorak et al. (1990) where percent differences are used is difficult because there is no way to tell how one translates to the other. This supports the idea that in the field of LBP due to instability, establishing a standard statistical technique for calculating a method's repeatability would be useful for comparison, along with a similar technique used for comparing the accuracy of studies.

Table 1: ICC values comparing repeatability of each technique as reported by Pearson et al. (2011) and Yeager et al. (2014).

ICC Values				
Study	**Intraobserver ICC(3,1)**		**Interobserver ICC(3,2)**	
	Translation	**Rotation**	**Translation**	**Rotation**
Pearson et al. (2011)	0.577-0.959	0.870-0.997	0.151-0.862	0.693-0.976
Yeager et al. (2014)	0.172-0.931	0.625-0.983	-0.019-0.820	0.551-0.958

CHAPTER 3: MATERIALS AND METHODS

3.1 Apparatus Fabrication

An apparatus was fabricated to allow one lumbar vertebral segment movement relative to another one (Figure 14). Fabrication was done in collaboration with a machinist. The vertebrae are able to move in five degrees of freedom: anterior-posterior translation, lateral translation, anterior-posterior rotation, lateral rotation, and axial rotation. The inferior vertebra is fixed to the bottom base plate by two screws drilled into its inferior endplate. The middle base plate is only permitted to move in the lateral direction through a well cut out on top of the bottom base plate. Once in position it is locked into place by set screws. The top base plate moves in the anterior-posterior direction through another well cut out on top of the middle base plate. It fits snuggly into this well which holds it in place. Each of the base plates has 10 mm of freedom in each direction. This allows for sufficient translation in each direction comparable to other cadaveric studies (Harvey et al., 1998; Shaffer et al., 1990), and also to encapsulate the accepted translations leading to lumbar instability (Pearson et al., 2011; Yeager et al, 2014). The middle and top base plates have holes cut through them to provide ample space for the inferior vertebra. Vernier scales were placed on the bottom and middle base plates to use for measuring the translations. These parts account for the desired translations of this study (Figure 15).

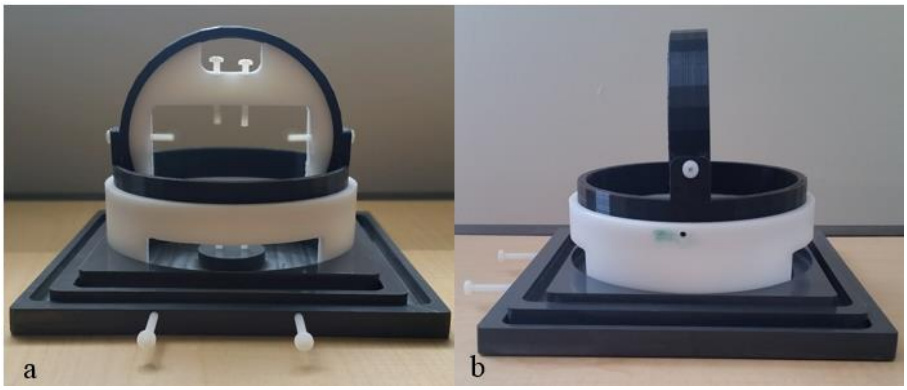

Figure 14: Fully assembled apparatus: (a) Front view of the complete apparatus, (b) Side view of the complete apparatus.

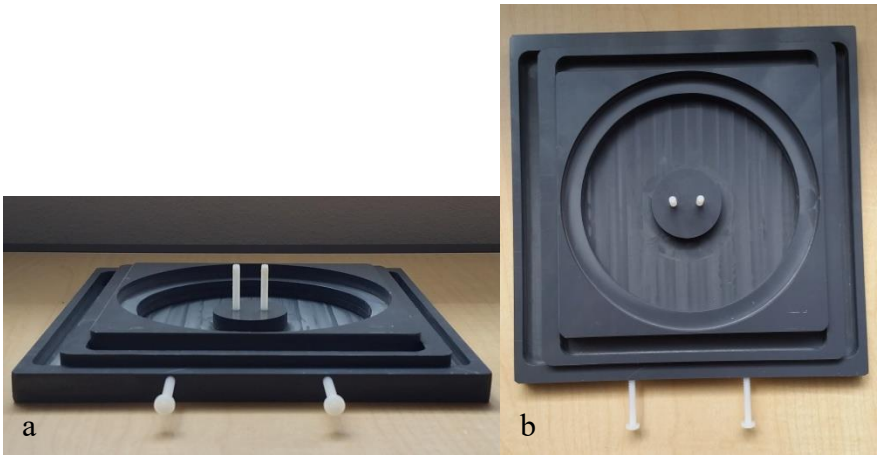

Figure 15: Apparatus base plates: (a) Front view of the three base plates, (b) Top view of the three base plates.

The three degrees of rotation occur using a collection of rings and clamps that allow the vertebrae to rotate freely in all directions. The inner clamp (Figure 16a) holds the superior vertebra rigidly fixed using two screws drilled into the superior endplate. An opening of 90 mm for the inner clamp was chosen based on measurements taken from a porcine vertebral specimen, in order to keep as many of the anatomical landmarks as possible. There are two indented grooves on the inner clamp's exterior that align with protruding grooves on the inside of the outer clamp (Figure 16b) allowing for lateral

rotation in the coronal plane. These two parts make up the inner-outer clamp assembly (Figure 16c).

Figure 16: Clamp assembly: (a) Inner clamp, (b) Outer clamp, (c) Inner-Outer clamp assembled.

The outer clamp sits inside the axial rotating ring (Figure 17a) using screws. This allows for anterior-posterior rotation of the inner-outer clamp assembly. Once in place, the screws are tightened to hold the assembly rigid. The axial rotating ring sits on a ledge on top of the top base ring (Figure 17b). This ring allows for axial rotation of 360^{o} in the transverse plane. Once in the desired position a set screw is used to hold it in place. The top base ring sits on top of the top base plate to provide the base for the axial rotating ring to perform its function. It was made 40 mm tall to afford enough space in the apparatus for two lumbar vertebrae motion segments, based on measurements taken from our porcine vertebral specimen. Windows were cut through the anterior and posterior portion of the ring in order to allow for better visualization of the vertebrae in the apparatus (Figure 17c and 17d). The collection of these parts allows for sufficient rotations in every direction comparable to other cadaveric studies (Bifulco et al., 2001; Breen et al., 1988; Cholewicki et al., 1991; Hanley et al., 1976; Shaffer et al., 1990), and also those

clinically seen to cause lumbar instability (Pearson et al., 2011; Yeager et al, 2014). All desired rotations for this study are accounted for in the design of these parts. An angular Vernier scale was placed on the rings and clamp assembly centered at the axis of rotation of the clamp that was used for measuring anterior-posterior rotations.

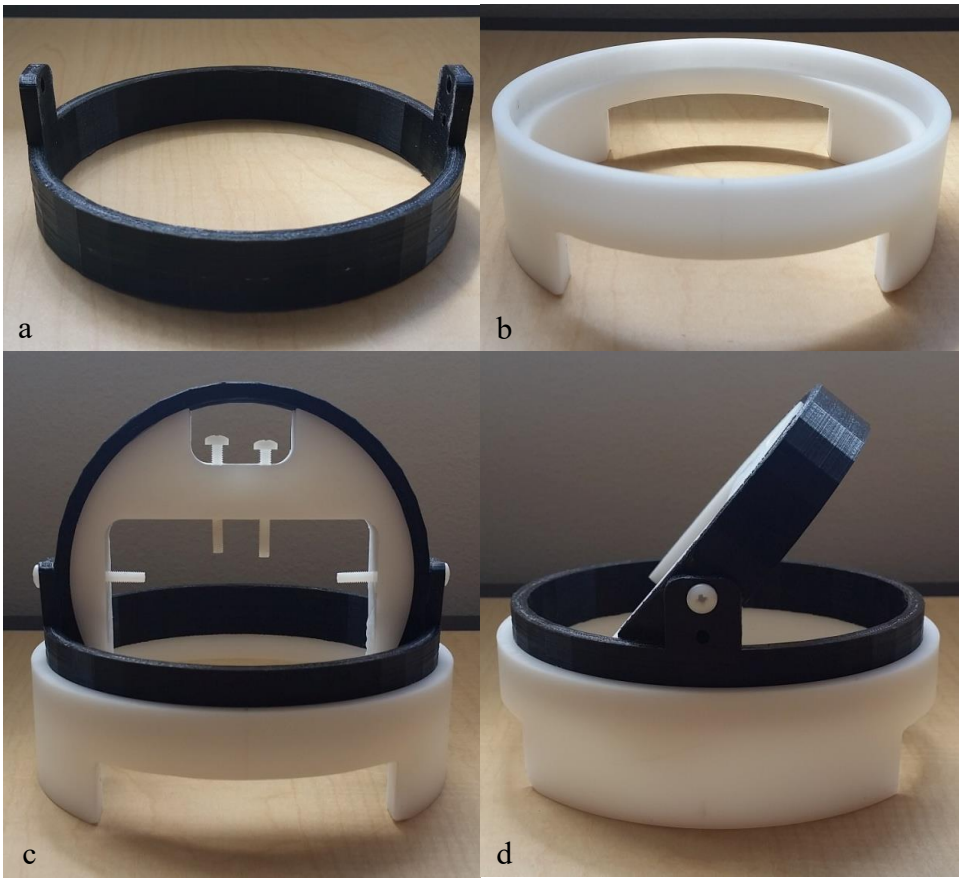

Figure 17: Rings and clamps assembly: (a) Axial rotating ring, (b) Top base ring, (c) Front view of rings and clamp assembly, (d) Side view of rings and clamp assembly.

The material for every part of the apparatus had to be carefully chosen for use in Magnetic Resonance Imaging (MRI). The MRI uses a large magnet in order to acquire its images, therefore any ferrous material could not be used. This would cause distortion of the images by altering the magnetic fields induced. It could also possibly damage the

machine because the strong attraction the magnet has for ferrous materials could pull the apparatus into the magnet. Additionally, the materials needed a high modulus of elasticity, or stiffness, in order to resist deformation once the parts have been set in their respective displacements. Movement after the parts have been set in place will be detrimental to measuring the accuracy of this study. From these factors, Polyvinyl Chloride (PVC), Delrin, and Polylactic Acid (PLA) were chosen for fabrication.

PVC was chosen for all three base plates because it is a stiff, inexpensive, and easy to machine material that the machinist had available. Delrin is a plastic with similar properties to PVC, nonferrous, stiff, and easy to machine, but is slightly more expensive. This material was used for the inner clamp and the top base ring. The outer clamp and axial rotating ring were 3-D printed with PLA using a MakerBot Printer (Brooklyn, New York) with the highest quality, 40% infill, and 5 shells to ensure high accuracy and stiffness. Also, nylon set screws were used because of their nonferrous characteristics and similar mechanical properties. This comprises the full details of the apparatus constructed.

3.2 Experimental Design

Two intact porcine spines were purchased from a local butcher. Porcine specimens were chosen because of availability, cost, and anatomical similarities to humans. Additionally, in comparison to human cadaveric vertebrae the pathogenic contact is reduced and guidelines for handling are less strict. Busscher et al. (2010) found that the sizes of human and porcine vertebral bodies are similar in the anterior and central portion, but porcine vertebral bodies were slightly smaller in the posterior portion.

Our experiment acquired images from the central portion of the vertebral body, justifying the use of porcine vertebrae. All vertebrae from both spines were dissected and disarticulated (Figure 18). Additionally, their processes were trimmed to allow for sufficient movement inside the apparatus.

Figure 18: Porcine vertebrae specimen: (a) Superior view of porcine vertebra, (b) Frontal view of porcine vertebra, (c) Frontal view of both porcine vertebrae.

The specimens were kept in a -30 ^{o}C freezer. On days when imaging was performed, they were removed from the freezer 3 hours prior to acquiring images in order to thaw. The inferior vertebra was mounted on the bottom base plate by two screws. The superior vertebra was set inside the inner-outer clamp assembly by two screws in the superior endplate (Figure 19). The vertebrae were misted with a saline solution every 30-45 minutes to keep the tissue from drying out. The vertebrae were imaged in a 0.25 Tesla open MRI (Esaote G-scan Brio, Genoa, Italy) torso coil (Figure 20).

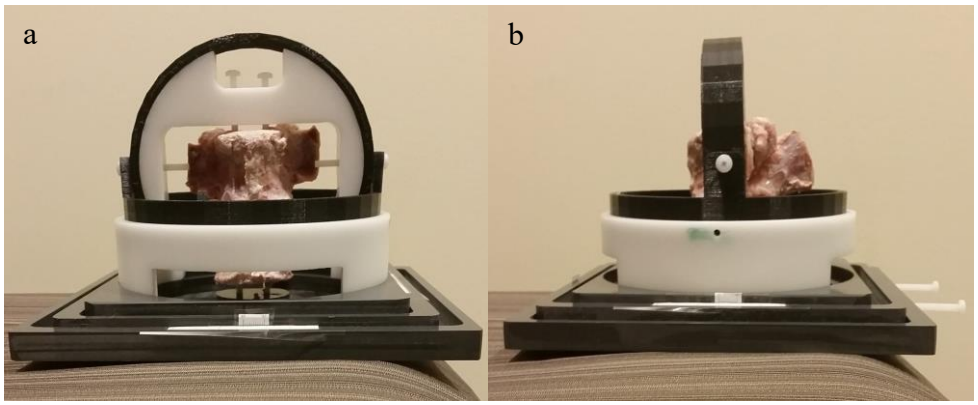

Figure 19: (a) Frontal view of porcine vertebrae in the apparatus, (b) Lateral view of porcine vertebrae in the apparatus.

Figure 20: Open-MRI used for imaging porcine vertebrae.

A wooden mount was built and secured in the center of the MRI coil by Velcro. This allowed for repeated removal and replacement of the apparatus in the same position between each successive trial during one day of imaging (Figure 21). The apparatus was placed into the mount for each trial and sand bags were placed on opposite sides of the mount to eliminate any movement from the vibration of the machine (Figure 22).

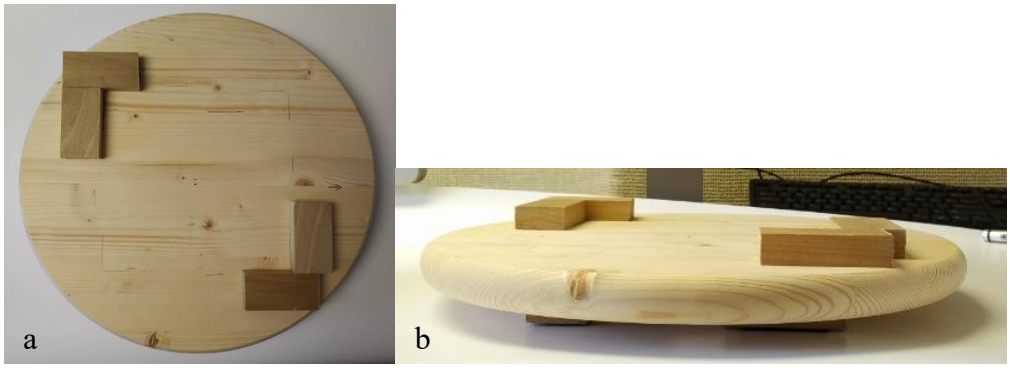

Figure 21: (a) Top-down view of the wooden mount used for positioning the apparatus in the MRI, (b) Side view of the wooden mount used for positioning the apparatus in the MRI.

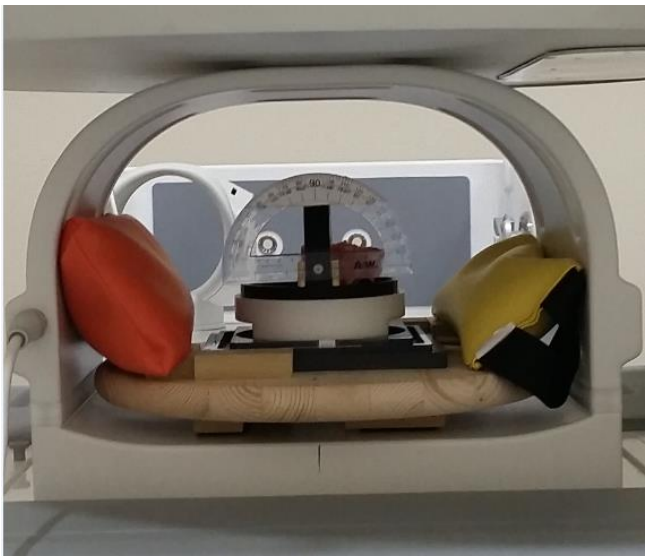

Figure 22: View of the apparatus in the mount attached to the MRI coil with sandbags for stabilizing.

Eight translations and rotations were chosen for both lateral bending and flexion-extension. The magnitudes were chosen based on similar cadaveric studies (Breen et al., 1988; Bifulco et al., 2001; Cholewicki et al., 1991; Hanley et al., 1976; Shaffer et al., 1990) and to account for displacements seen clinically (Dvorak et al., 1991; Hanley et al., 1995; Hayes et al., 1989; Pearcy et al., 1984; Pearson et al., 2011; White and Panjabi, 1978; Yeager et al, 2014). The values were randomly chosen without replacement in

order to eliminate any unintended bias when measuring a specific displacement. In order to ensure an evenly spread data set, each translation and rotation was broken up into bins in increments of 5 mm or degrees, respectively (Table 2). The translational magnitudes for both lateral bending and flexion-extension ranged from -5 to 5 mm. The rotational magnitudes for lateral bending ranged from -10 to 10 degrees, and for flexion-extension they ranged from -5 to 15 degrees. The random displacements for imaging are shown in the diagrams in Figure 23. The displacements chosen were then randomized and imaged in that order.

Table 2: Number of displacements without replacement per bin for each movement.

Relative Vertebral Displacements							
Movement	**Translation (mm)**		**Rotation (degrees)**				
	-5 to -1	1 to 5	-10 to -6	-5 to -1	1 to 5	6 to 10	11 to 15
Lateral Bending	4	4	2	2	2	2	-
Flexion-Extension	4	4	-	2	2	2	2

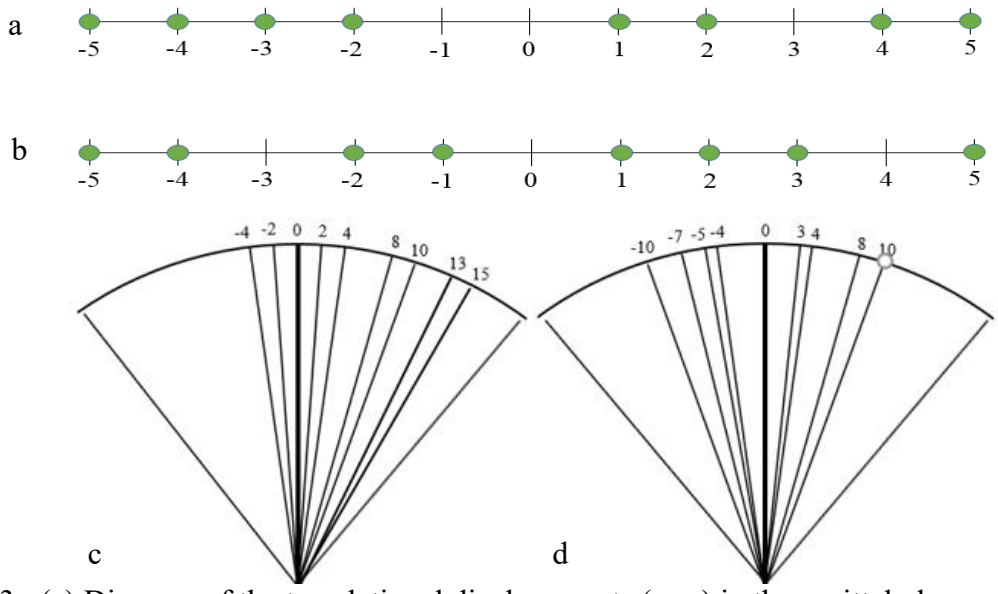

Figure 23: (a) Diagram of the translational displacements (mm) in the sagittal plane indicated by the green dots, (b) Diagram of the translational displacements (mm) in the coronal plane indicated by the green dots, (c) Rotational displacements (degrees) in the sagittal plane indicated by each line, (d) Rotation displacements (degrees) in the coronal plane indicated by each line. (Diagrams not to scale)

This resulted in 16 total translations and 16 total rotations of the top vertebra relative to the bottom. Two sets of images were acquired: one using a 2D HYCE S dynamic sequence (2-dimensional hybrid contrast enhanced streaming sequence; resolution = 0.98 mm, thickness = 8 mm, slice = 1, scan time = ~10s/scan) and another using a T1 static sequence (resolution = 0.78 mm, TR = 810 ms, TE = 30 ms, FOV = 220 x 220, Matrix = 256 x 256, slices = 3, gap = 0, thickness = 5 mm, scan time = ~2 mins/scan). Figure 24 shows sample images of both sequences that were acquired during the study. This process was done with two sets of porcine vertebrae, in order to see if there was variability between the segments. The two segments were chosen from two different porcine spines at two different levels because the adjacent level vertebrae from the opposite spines were used in initial failed trial runs which rendered the tissues no

longer usable. Lumbar vertebrae 5 and 6 were used for the first trials and lumbar vertebrae 3 and 4 were used for the second trials. Pigs have six lumbar vertebrae compared to humans who normally have five.

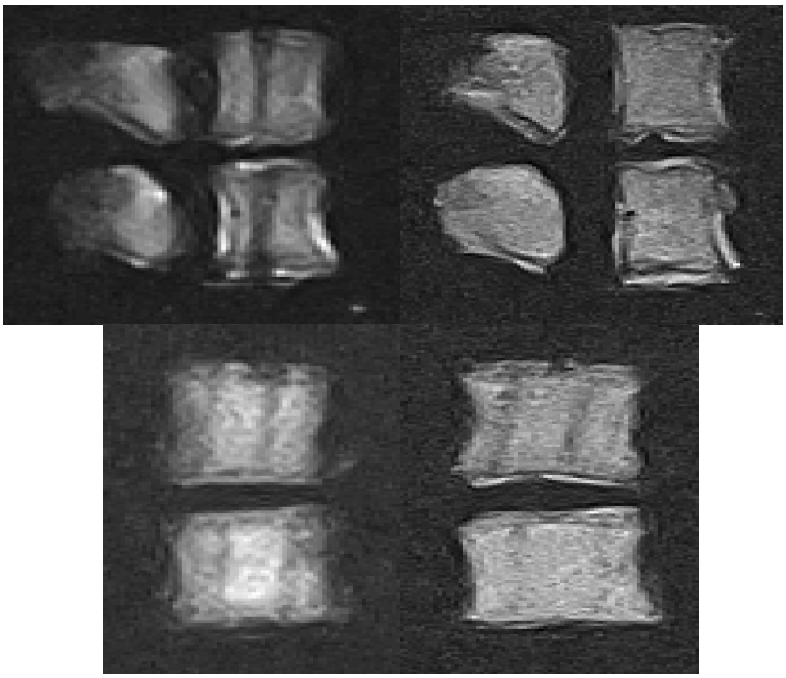

Figure 24: MR images of the porcine vertebrae obtained with the setup of this study. (Top images = sagittal plane, bottom images = coronal plane, left images = 2D HYCE S sequence, right images = T1 sequence)

Eight separate sessions were conducted in order to acquire all necessary images ([16 translations + 16 rotations] * 2 spine segments * 2 image sequences = 128 images). Each session used both imaging sequences for either the translation or rotation displacements of one movement, either lateral bending or flexion-extension. Each session the MRI and lumbar coil were calibrated. The porcine vertebrae were then secured in the apparatus which was then placed into the mount and secured with sandbags. The vertebrae were initially placed in a neutral position and imaged. This was

used to establish a baseline value of neutral to compare the subsequent images back to in order to calculate the relative displacements. For each desired translational and rotational displacement the apparatus was removed from the MRI room and the subsequent displacement was implemented. The schedule for collecting all the images is shown in Table 3.

Table 3: The schedule showing the days imaging was performed and the spine, movement, and plane that was imaged during each session.

Schedule for Imaging of Porcine Vertebrae			
Date	**Spine**	**Movement**	**Plane**
6/15/2015	L5-6	Translation	Sagittal
6/16/2015	L3-4	Translation	Coronal
6/18/2015	L5-6	Translation	Coronal
6/19/2015	L3-4	Translation	Sagittal
6/22/2015	L5-6	Rotation	Sagittal
6/23/2015	L3-4	Rotation	Sagittal
6/24/2015	L5-6	Rotation	Coronal
6/25/2015	L3-4	Rotation	Coronal

Once all images were acquired, they were saved in a DICOM format in a folder labeled with the day and imaging code describing the trial. The imaging code consisted of two letters and a number. The first letter was either "S" for a sagittal view or "C" for a coronal view. The second letter was either a "T" for a translational displacement or "R" for a rotational displacement. Lastly, the number was either "1" for spine segment 1 or "2" for spine segment 2 for example, Day 1 – ST1. The respective images within each folder were then randomized again and assigned a letter from "A" through "I" for a blinded analysis. The DICOM files were then opened in Matlab.

In Matlab, a code developed in collaboration with Dr. Cotton for this study was run one image at a time to select data points on all 128 images. The code opens all DICOM images in a selected folder. The observer is then prompted to select the four corner points of the bottom vertebra starting in the bottom left corner and proceed counterclockwise. After the four corners have been selected, the observer presses "Enter" and repeats the process for the top vertebra. To move on to the next image, "Enter" is pressed again. Once all images have been viewed, the program will stop and save one file of the raw data points.

The manual selection of the four corner points of both vertebra is shown in Figure 25. In addition to the four-point selection technique, a separate trial was run with the observer selecting six points on each vertebral body. This was done only for analyzing the rotational displacements to explore if the accuracy of the measurements would improve by adding additional data points. The observer starts in the bottom left corner and proceeds counterclockwise again but this time selects an additional midpoint on both the bottom and top endplates of each vertebral body. During selection of the points the observer is blind to what is the actual displacement. This process was done on two separate days for both point selection techniques: the first day consisted of analyzing all images for the L5-6 segment and the second day consisted of analyzing all the images for the L3-4 segment. The image analysis was repeated two weeks later in the same manner by the same observer. Also, a second observer (a fellow medical student) performed the four-point selection technique in the exact same manner. This was done on the same

images on two separate days. The data was used to provide a comparison of the accuracy and repeatability of the method between different observers.

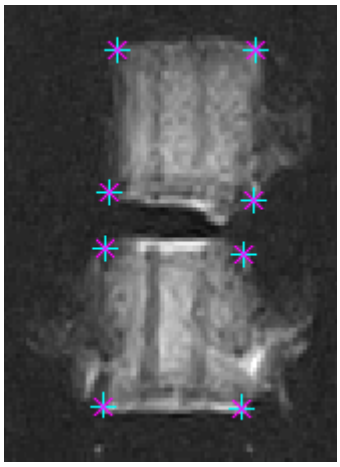

Figure 25: Ex vivo image of the porcine vertebrae in the apparatus showing the technique of selecting the four corner points on each porcine vertebra.

From these data points, the Matlab program calculated the translations and rotations of the superior vertebra relative to the inferior. The "x" (or "z") and "y" position was the average of the data points selected on the individual vertebra. The displacements of the superior vertebra were measured in reference to the inferior vertebra's position. The translations were calculated by measuring the change along the horizontal axis, ΔX in the coronal plane and ΔZ in the sagittal plane (Breen et al., 1988 and Fujii et al., 2007), between the midpoints of the two vertebral bodies (L_{i-1} and L_i) (Figure 26).

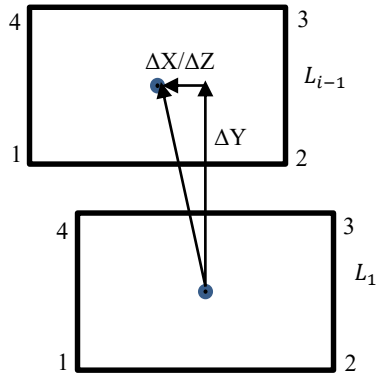

Figure 26: Diagram of calculating translational displacements, ΔX in the coronal plane and ΔZ in the sagittal plane, between the vertebrae.

From the data points selected on each vertebra a slope of the line on the top endplate and the line on the bottom endplate was calculated. The slopes were then averaged for each vertebra *(L_{i-1}* and L_i). The relative rotation between the vertebra, α, was then calculated as the inverse tangent of the difference of the slopes between the two vertebra (Figure 27). This information is saved by the Matlab code into one file with all the displacements calculated for each image. The displacements calculated are the angle of the top vertebra, angle of the bottom vertebra, relative angle between the top and bottom vertebra, translation in the horizontal axis, and translation in the vertical axis.

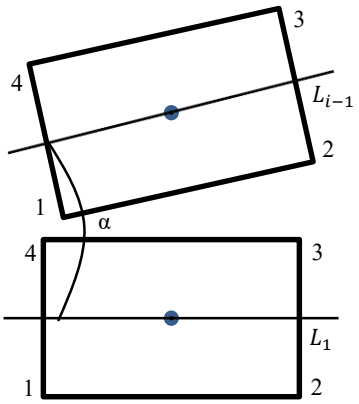

Figure 27: Diagram of calculating rotational displacements between vertebrae.

These measurements calculated from the manual MRI point selection techniques were compared to the physically measured translations and rotations of the vertebra in the apparatus. RMS error is the most consistently reported statistic in the literature (Cholewicki et al., 1991; Ishii et al., 2004; Pearcy and Whittle, 1982; Stokes et al., 1981; Wang et al., 2008). Therefore, these values were calculated for comparison to similar studies. Standard error of the estimate (SEE) values were also calculated. The SEE is more applicable to our data and regression lines rather than comparing to a mean value. A linear regression model was run in the statistical analysis software *R* (Version 3.3.1, The R Foundation for Statistical Computing, Vienna, Austria, 2016). This was used to determine the significance of different variables (spine segment, day, imaging sequence, and image orientation) on the outcome of the accuracy and repeatability of the manual point selection techniques. It was also used for analyzing the adjusted R^2 values along with the slopes and intercepts of the trend lines for each trial. Finally, intraclass correlation coefficient (ICC) values were calculated as stated by Shrout and Fleiss (1979) using SPSS (Version 21, IBM, Armonk, NY). This was done for comparison of one

observer performing the point selection technique on multiple days (intraobserver), in this study it was two days. The value is reported as ICC(2,1) meaning it is model 2 with one observer. Model 2 was chosen because it is the least conservative. Unlike model 3, which was used by Pearson et al., 2011 and Yeager et al., 2014, it represents the repeatability of the process for the general population and makes no assumptions about the rater or subjects measured being fixed. Model 3 calculates the repeatability for the specific individual performing the task assuming they doesn't represent the general population. These values were also calculated for comparison between two observers (interobserver) performing the point selection technique on the same series of images. The value is reported as ICC(2,2) meaning it is again model 2 but now with two observers. These values show the repeatability of the point selection technique. Altogether, this data determines the accuracy and repeatability of this technique and study for use in future in vivo studies.

CHAPTER 4: RESULTS

4.1 Translational Displacements

The translational measurements for each imaging sequence and plane combination were plotted and compared to the actual translations of the apparatus (Figure 28). Similarly, the RMS errors associated with each graph were calculated (Table 4). These errors represent the differences in the measured displacements using the point selection technique from the actual displacements of the apparatus.

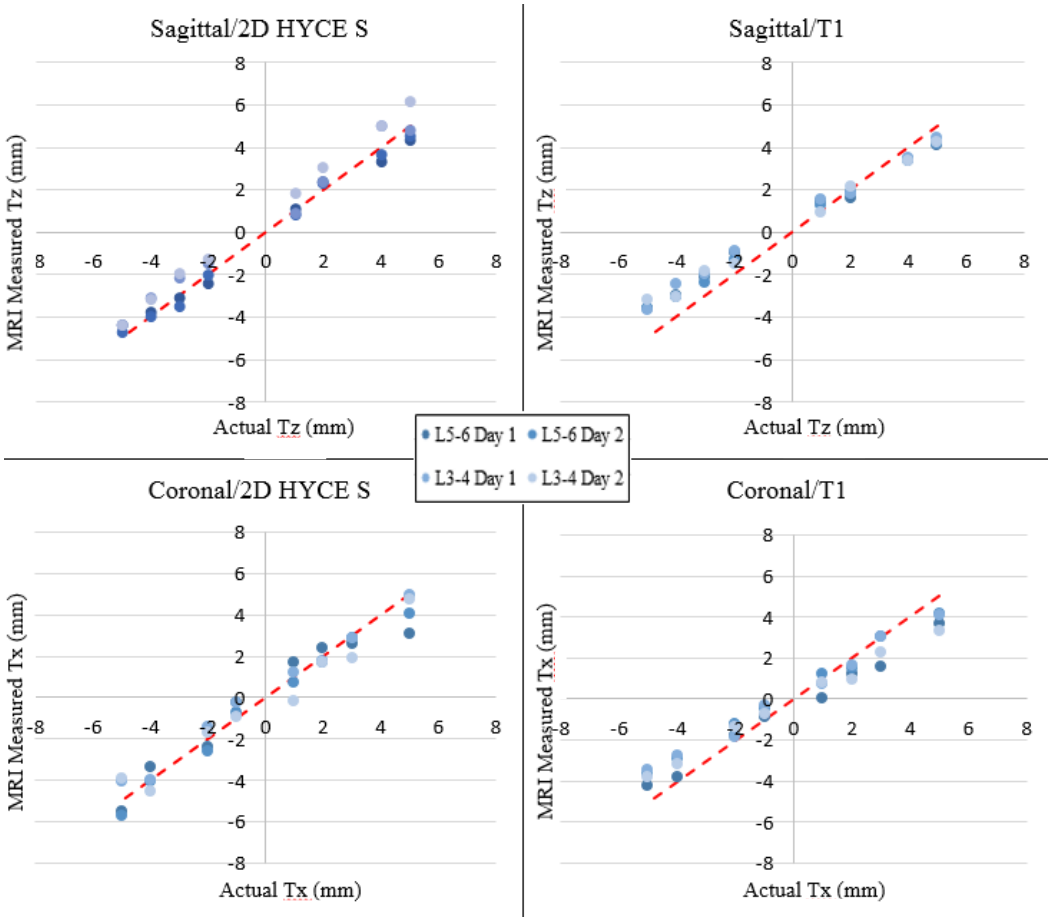

Figure 28: Graphs showing the translational measurements from MRI scans compared to the translations measured in situ for the sagittal plane (top graphs) and coronal plane (bottom graphs) and the two different MRI sequences: 2D HYCE S (left graphs) and T1 (right graphs). (The dashed red lines represent y = x)

Table 4: Table of RMS errors (difference between measured and actual displacements) of all the measurements obtained from the MRI images of the porcine vertebrae.

Plane	Sequence	RMS Error (mm)
Sagittal	T1	0.89
	2D HYCE S	0.65
Coronal	T1	0.86
	2D HYCE S	0.66

The linear regression analysis run using the statistical analysis software *R* found a statistically significant regression model ($p<0.001$) (Appendix A). The coefficient of

determination, or adjusted R^2 value was 0.97. From the model it was found that the sequence and day were not statistically significant predictors of the variance ($p>0.05$). The model was run again excluding these two variables. The new regression model was found to be statistically significant ($p<0.001$) (Appendix A). The adjusted R^2 value remained 0.97.

From this output, the intercept, measured displacement (MD), coronal plane (CorPlane), and spine segment 1 (Spine1) are significant variables. The intercept has a value of -0.56, β_0, which is used to predict the bias. The MD has a value of 1.13, β_1, which is the slope of the regression line fit to this model. The CorPlane has a value of 0.44, β_2, and Spine1 has a value of 0.36, β_3. The variables that were not found to show significance were the 2D HYCE S sequence (HySeq) or Day 1 (Day1). The following model for predicting the set displacement of the apparatus (SD) was generated from these significant variables and the random error, *e*, or residual:

$$SD = \beta_1 MD + \beta_2 CorPlane + \beta_3 Spine1 + \beta_0 + e$$

This model can be used to predict any measurement by giving the statistically significant variables a value of 1 if they are present. The overall standard error, the error between MD and the regressed model, was 0.61 mm.

The standardized beta coefficients, shown in Table 5, were also calculated. This was done by individually dividing the standard deviation of each predictive or significant variable (MD, CorPlane, and Spine1) by the standard deviation of the outcome, SD, resulting in the unstandardized coefficient. The unstandardized coefficient is then multiplied by the β coefficient for each variable giving the standardized beta coefficient.

This shows the relative influence each variable has on the displacements of the apparatus. The measured displacement has the greatest relative impact on the variance with a value of 0.987. This value is a way of weighting the impact each variable has on the variance of the model, with 1.00 encompassing all of the influence on the variance. Although very small, the coronal plane and spine 1 have an impact on the variance seen in the model, 0.065 and 0.053 respectively. Another way to reiterate the impact each variable has on the regression model is to calculate the impact each variable has on the standard error when it is added to the model. This progression is shown in Table 6.

Table 5: Table of standardized beta coefficients for the statistically significant variables in the regression model.

Variables	**Standardized Beta Coefficients**
Measured Displacement	0.987
Coronal Plane	0.065
Spine 1	0.053

Table 6: Table showing the standard errors and the relative changes when each variable is added to the regression model.

Variables	**Standard Error (mm)**	**Change in Standard Error (mm)**
Measured Displacement	0.67	-
Measured Displacement + Coronal Plane	0.63	0.04
Measured Displacement + Coronal Plane + Spine 1	0.61	0.02

Table 6 shows that alone the measured displacement has the highest standard error. By adding the coronal plane to the model it only reduces the standard error by 0.04 mm. Lastly, by adding the last significant variable of spine 1 it only reduces the error by

0.02 mm. This again demonstrates the small impact that the coronal plane and spine have on the study. They decrease the error of the study by only a total of 0.06 mm, which is almost negligible.

The Intraclass Correlation Coefficients (ICC) values were also calculated for each plane and MRI sequence as stated by Shrout and Fleiss (1979) using SPSS. This data is shown in Table 7. All ICC values for both intra and interobserver were above 0.925 which shows a high level of agreement within and between observers. The lowest 95% CI was 0.853 for ICC(2,2) for the sagittal plane and T1 sequence which still demonstrates a high degree of agreement.

Table 7: Table of ICC values and their 95% confidence intervals (CI) for comparison of the point selection technique within observers (intraoberserver) and between observers (interobserver) for each plane and sequence.

		Intraobserver			**Interobserver**		
Plane	**Sequence**	**ICC(2,1) Value**	**Lower 95% CI**	**Upper 95% CI**	**ICC(2,2) Value**	**Lower 95% CI**	**Upper 95% CI**
Sagittal	T1	0.995	0.987	0.998	0.925	0.853	0.962
	2D HYCE S	0.993	0.983	0.998	0.972	0.945	0.986
Coronal	T1	0.981	0.950	0.993	0.961	0.925	0.980
	2D HYCE S	0.988	0.966	0.995	0.976	0.952	0.988

4.2 Rotational Displacements

The rotational measurements for each imaging sequence and plane combination for both the four and six-point selection techniques were plotted and compared to the actual rotations of the apparatus (Figure 29 and 30, respectively). Similarly, the RMS errors associated with each graph were calculated (Table 8).

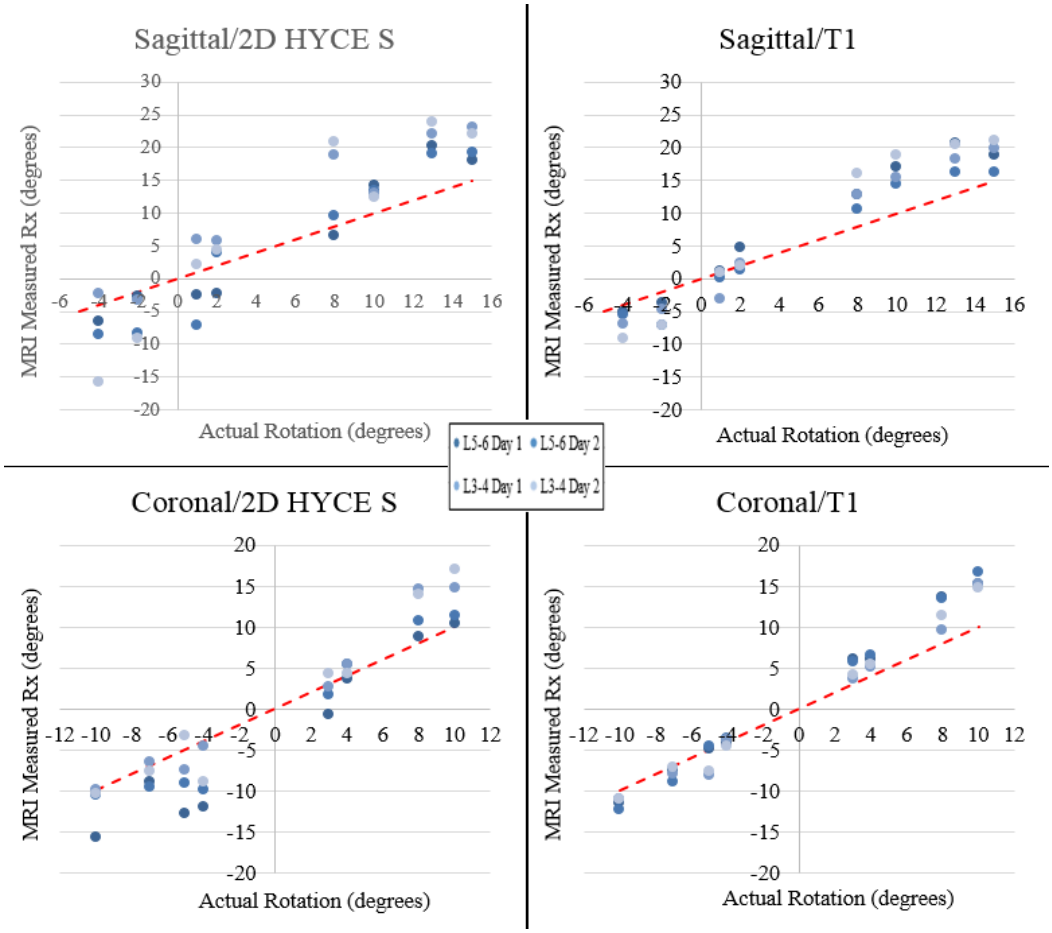

Figure 29: Graphs showing the rotational measurements calculated from the four-point selection technique from MRI scans compared to the rotations measured in situ for the sagittal plane (top graphs) and coronal plane (bottom graphs) and the two different MRI sequences: 2D HYCE S (left graphs) and T1 (right graphs). (The dashed red lines represent y = x)

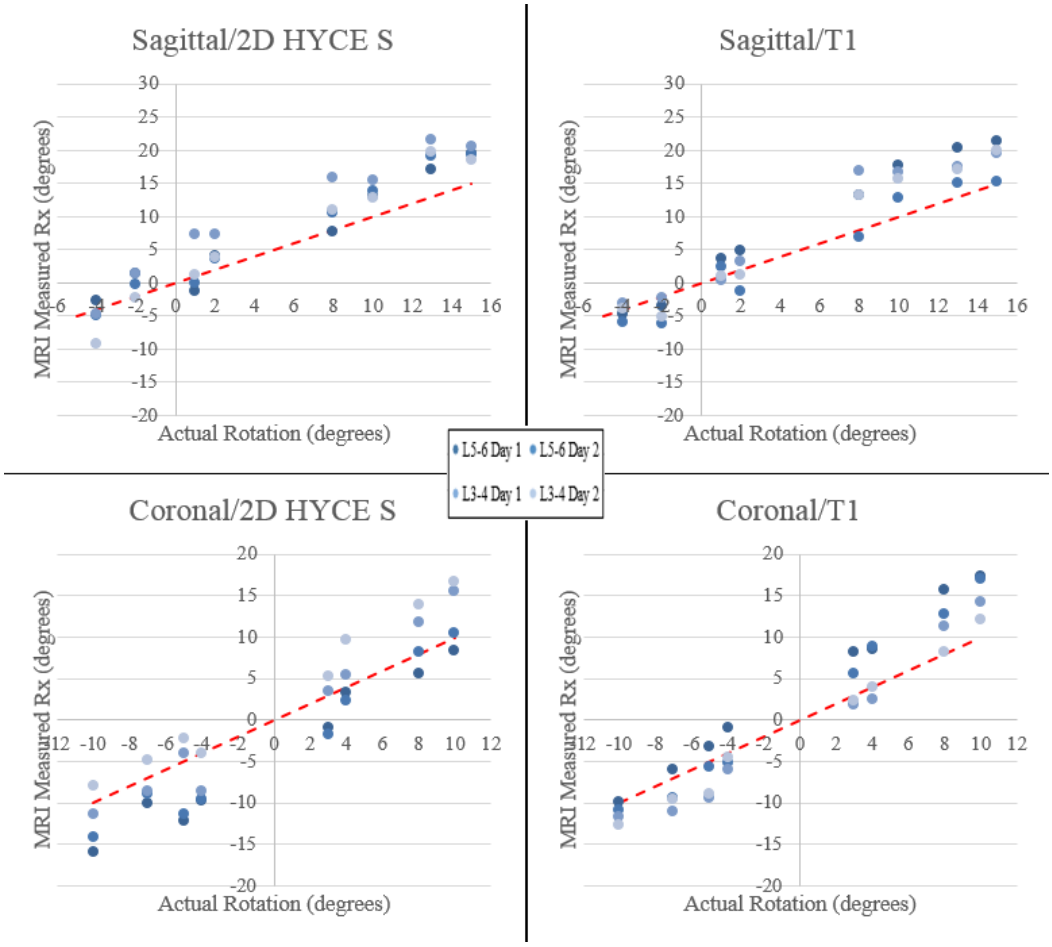

Figure 30: Graphs showing the rotational measurements calculated from the six-point selection technique from MRI scans compared to the rotations measured in situ for the sagittal plane (top graphs) and coronal plane (bottom graphs) and the two different MRI sequences: 2D HYCE S (left graphs) and T1 (right graphs). (The dashed red lines represent y = x)

Table 8: Table of RMS errors of all the measurements obtained from the MRI images of the porcine vertebrae for both the four and six-point selection technique.

		RMS Error (degrees)	
Plane	**Sequence**	**Four-Point Selection Technique**	**Six-Point Selection Technique**
Sagittal	T1	4.90	4.04
	2D HYCE S	6.63	4.09
Coronal	T1	2.98	3.54
	2D HYCE S	3.79	3.85

Separate linear regression analyses were run for the four and six-point selection technique of measuring rotational displacements using the statistical analysis software *R*. This was done in the same manner as the translational measurements. Both techniques had statistically significant regression models ($p<0.001$) (Appendix B). The adjusted R^2 values for each technique were 0.93. From the models it was found that for the four-point selection technique, similar to the translational displacements regression model, the sequence and day were not statistically significant predictors of the variance ($p>0.05$). However, for the six-point selection technique the only statistically significant variable was the point selection technique. Both these models were run again with only the statistically significant variables remaining. The new regression models were found to be statistically significant ($p<0.001$) (Appendix B). The adjusted R^2 values were again 0.93 for both methods.

From these outputs neither intercept is significant. The four-point selection technique was found to have the following significant variables: measured displacement (MD), coronal plane (CorPlane), and spine segment 1 (Spine1). The MD has a value of 0.64, β_1, which is the slope of the regression line fit to this model. The CorPlane has a value of -1.09, β_2, and Spine1 has a value of 0.99, β_3. The variables that were found to not show significance were the 2D HYCE S sequence (HySeq) or Day 1 (Day1). The following model for predicting the set displacement of the apparatus (SD) was generated from these significant variables and the random error, *e*, or residual:

$$SD = \beta_1 MD + \beta_2 CorPlane + \beta_3 Spine1 + e$$

The six-point selection technique was only found to have one significant variable, MD with a value of 0.69. All other variables were found to not show significance. As before, the following model for predicting the SD was generated:

$$SD = \beta_1 MD + e$$

These models can be used to predict any measurement for the respective technique by giving the statistically significant variables a value of 1 if they are present. The overall standard errors, the error between MD and the regressed model, were 1.93 and 2.00 degrees, respectively.

The standardized beta coefficients for each technique, shown in Table 9, were also calculated as done with the translational displacements. Again this shows the relative influence or weighted significance each variable has on the displacements of the apparatus. The measured displacement has the greatest impact on the variance for both the four and six-point technique with values of 0.943 and 0.967, respectively. Although very small, for the four-point selection technique the coronal plane and spine 1 have an impact on the variance seen in the model. Conversely, for the six-point selection technique there are no other variables beside the measured displacement that have an impact on the variance in the model. Another way to reiterate the impact each variable has on the regression model is to calculate the impact each variable has on the standard error when it is added to the model. This progression is shown in Table 10.

Table 9: Table of standardized beta coefficients for both the four and six-point selection technique for the statistically significant variables in the respective regression models.

	Standardized Beta Coefficients	
Variables	**Four-Point Selection Technique**	**Six-Point Selection Technique**
Measured Displacement	0.943	0.967
Coronal Plane	-0.074	-
Spine 1	0.068	-

Table 10: Table showing the standard error values and the relative changes when each variable is added to the regression model for both the four and six-point selection technique.

	Four-Point Selection Technique		**Six-Point Selection Technique**	
Significant Variables	**Standard Error (degrees)**	**Change in Standard Error (degrees)**	**Standard Error (degrees)**	**Change in Standard Error (degrees)**
Measured Displacement	2.04	-	2.00	-
Measured Displacement + Coronal Plane	1.98	0.06	-	-
Measured Displacement + Coronal Plane + Spine 1	1.93	0.05	-	-

Table 10 shows that alone the measured displacement has the highest standard error for both techniques. By adding the coronal plane to the model for the four-point selection technique it only reduces the standard error by 0.06 degrees. Lastly, by adding the last significant variable of spine 1 it only reduces the error by 0.05 degrees. This again demonstrates the small impact that the coronal plane and spine have on the study. They decrease the error of the study by only a total of 0.11 degrees which again is almost negligible. For the six-point selection technique there are no other statistically significant variables beside the measured displacement so therefore it is the sole variable that contributes to the standard error of the study.

The Intraclass Correlation Coefficients (ICC) values were also calculated for each plane and MRI sequence as stated by Shrout and Fleiss (1979) using SPSS. The second observer only performed the four-point selection technique so therefore there are no ICC(2,2) values for the six-point selection technique. This data is shown in Table 11. All ICC values for both intra and interobserver were above 0.819 which shows a high level of agreement within and between observers. The lowest 95% CI was 0.644 for ICC(2,2) for the sagittal plane and 2D HYCE S sequence which still demonstrates a moderate degree of agreement.

Table 11: Table of ICC values and their 95% confidence intervals (CI) for comparison of the four and six-point selection technique within observers (intraoberserver) and between observers (interobserver) for each plane and sequence.

		Four-Point Selection Technique					
		Intraobserver			**Interobserver**		
Plane	**Sequence**	**ICC(2,1) Value**	**Lower 95% CI**	**Upper 95% CI**	**ICC(2,2) Value**	**Lower 95% CI**	**Upper 95% CI**
Sagittal	T1	0.984	0.957	0.994	0.891	0.765	0.947
	2D HYCE S	0.959	0.893	0.985	0.819	0.644	0.908
Coronal	T1	0.998	0.995	0.999	0.930	0.805	0.970
	2D HYCE S	0.982	0.952	0.993	0.927	0.857	0.963
		Six-Point Selection Technique					
Sagittal	T1	0.967	0.791	0.990	-	-	-
	2D HYCE S	0.972	0.920	0.990	-	-	-
Coronal	T1	0.987	0.965	0.995	-	-	-
	2D HYCE S	0.982	0.924	0.994	-	-	-

CHAPTER 5: DISCUSSION

5.1 Translational Displacements

The results of this study show a strong correlation between the measured and actual values for the translations of the vertebrae (adjusted R^2 value = 0.968, average RMS Error = 0.77 mm). The predictive regression model for our manual point selection technique in Matlab is accurate (SEE = 0.61 mm). It is also a repeatable method of measuring translational displacements imaged using upright-MRI (Average ICC(2,1) = 0.989). Establishing the accuracy of this method facilitates its use in future studies. Further studies might use this method to analyze the kinematics of the lumbar vertebrae of patients with and without LBP to further understand its causes and most efficacious forms of treatment.

The RMS error in this study is comparable to others of its kind (Table 12). The average RMS error using the 2D HYCE sequence is 0.66 mm compared to 0.88 mm using the T1 sequence. These numbers indicate there are errors of 0.66 mm and 0.88 mm from the actual displacement of the apparatus when using our point selection technique with the 2D HYCE S and T1 sequences, respectively. Running this study with two different MRI sequences was done to see whether or not the 2D HYCE S sequence, although able to capture images in motion, would detract from the accuracy of our method. Overall, this study finds no loss of accuracy when using this sequence compared to the T1 sequence. The regression analysis shows that the 2D HYCE S sequence did not have any significant effects on the variance of the model compared to the standard T1 sequence, used for static imaging. This is beneficial for future studies using an upright

MRI to image and analyze physiological motion because it can only be done with specific dynamic imaging sequences such as the 2D HYCE S sequence used in this study.

Table 12: Table comparing the RMS errors for the translational displacements in the present study compared to similar studies found in the literature.

Study	Imaging Modality	RMS Error (mm)
Present Study	Upright-MRI	0.65-0.89
Stokes et al. (1981)	Biplanar Radiography	0.77-1.53
Pearcy and Whittle (1982)	Biplanar Radiography	0.17-2.07
Cholewicki et al. (1991)	3D Videofluoroscopy	0.46
Ishii et al. (2004)	3D MRI	0.41-0.52
Wang et al. (2008)	3D Videofluoroscopy	0.2-0.4

The majority of the studies in the literature use biplanar radiography (Stokes et al. 1981 and Pearcy and Whittle 1982) or 3D Videofluoroscopy (Cholewicki et al. 1991 and Wang et al. 2008). These imaging modalities have proven to be the most precise methods because of their enhanced image quality. Ishii et al. (2004) is the only study that used MRI, but their magnet strength was a 1.0 Tesla compared to our 0.25 Tesla. They also used ceramic ball markers to enhance their point selection. Although Ishii et al. (2004) has slightly smaller errors than our study, our design is more applicable to in vivo use due to the absence of markers.

The linear regression analysis provides further details about the accuracy of the translational measurements. Three variables were found to be statistically significant and account for 96.8% of the variance based on the adjusted R^2 value of 0.968: point selection technique, plane, and spine. However, the plane and spine only accounted for 0.7% of the 96.8% meaning they have an almost negligible influence on the variance. This is supported by the point selection technique having a much higher standardized

beta coefficient (0.987) compared to the plane and spine (0.065 and 0.053, respectively). Furthermore, the average RMS errors in the sagittal and coronal plane are almost identical (0.77 mm and 0.76 mm, respectively) supporting the fact that the plane is almost a negligible variable.

The reasons for the plane of viewing the image (coronal or sagittal) having a slight impact on the variance found in the model may be due to the dimensions of the vertebral body in each plane. When viewing from the coronal plane the vertebral body is wider and has a more rectangular shape. When viewing from the sagittal plane the vertebral body is slender and the anterior and posterior sides appear more concave in which may make picking the corner points more difficult. Also, the amount of tissue left on the vertebrae may appear different in each plane causing error in picking the correct location of each corner point.

As stated earlier, the spine segments used were from different porcine spines and different levels of the lumbar region (L3-4 and L5-6). The standardized model shows that this does have a slight influence on the variance of the model similar to the plane, however it is minimal (standardized beta coefficient = 0.053, change in SEE = 0.02 mm). Our use of porcine vertebrae rather than human vertebrae is another possible limitation of this study. Although similar, there are slight differences between the vertebral body anatomy of the two which may have resulted in inconsistent selection of the corner points. The fact that the influence is rather minimal means that our method has the potential to be applicable to many different segments throughout the spine. In future

similar studies, segments from two different spines at the same levels should be evaluated to see whether or not the influence of the spine is completely resolved.

Further data from the regression model is the significance of the intercept and the slope of the measured displacement variable and the standard error of 0.61 mm. The intercept has a value of -0.565 meaning there is some bias in the method that is underestimating the translations by 0.565 mm overall. The slope of the measured displacement (MD) regression line is 1.13. Ideally the slope would be 1 indicating a 1:1 relationship between the measured and actual displacements. The standard error of 0.61 mm means that a measurement of translational movement estimated from the regression formula is within ±1.22 mm with 95% certainty.

In regards to the repeatability of measuring translational displacements with our point selection technique, the ICC values for both intraobserver and interobserver shown in Table 13 show very strong agreement. All the values are greater than 0.925 with many of them showing an almost near perfect agreement of 1. Table 10 shows the ICC values from this study compared to other values reported in the literature. Our values are comparable and even better than some studies using similar manual measuring techniques. Similarly, our values are comparable to studies using computer-assisted methods. From the regression model the day of performing the point selection technique was found to have no statistically significant influence on the variance of the model. This demonstrates that our method is highly repeatable for one person or multiple people performing the point selections.

Table 13: Table comparing the ICC values obtained for the translational displacements in the present study to similar studies found in the literature.

ICC Values				
Study	**Manual or Computer-Assisted**	**Model**	**Intraobserver ICC**	**Interobserver ICC**
Present Study	Manual	2	0.981-0.995	0.925-0.976
Teyhen et al. (2005)	Manual	2	0.966-0.993	0.637-0.944
Fritz et al. (2005)	Manual	2	0.84-0.99	-
Pearson et al. (2011)	Manual	3	0.083-0.866	-0.122-0.780
Pearson et al. (2011)	Computer-Assisted	3	0.741-0.990	0.343-0.962
Yeager et al. (2014)	Manual	3	0.625	0.551
Yeager et al. (2014)	Computer-Assisted	3	0.983	0.958

Implementing an accurate method of measuring the kinematics of the lumbar spine helps clinicians understand how the vertebrae are moving in order to quantify different pathologies which aids in the diagnosis and treatment of LBP. The movements of the vertebrae relative to one another during specific movements occur in incrementally small measurements (translations measured in millimeters and rotations measured in degrees). Therefore, high accuracy and repeatability of these measurements is desired because small errors will lead to incorrect measurements and inappropriate diagnoses of instability causing LBP.

5.2 Rotational Displacements

The results of this study show a weaker correlation (adjusted R^2 values = 0.931 and 0.926, average RMS error = 4.58 and 3.88 degrees) between the measured and actual values for the rotations of the vertebrae, when compared to the translational

measurements, for both the four and six-point selection techniques, respectively. The accuracies of the predictive regression models for the rotational displacements are also diminished compared to the translational measurements (SEE = 1.93 and 2.00 degrees, respectively). However, the repeatability remains strong for both the four and six-point selection techniques (Average ICC(2,1) = 0.981 and 0.977, respectively). Continued work should be conducted to reduce the error and increase the accuracy of the method for measuring rotational displacements.

The overall average RMS error is smaller for the six-point technique, 3.88 degrees, compared to the four-point technique, 4.58 degrees, meaning there is more error in the measured rotations compared to the actual rotations of the apparatus for the four-point technique compared to the six-point technique. However, the average RMS errors in the coronal plane for both the four-point technique (RMS error = 3.39 degrees) and the six-point technique (RMS error = 3.70 degrees) are smaller relative to those in the sagittal plane (RMS error = 5.77 and 4.07 degrees, respectively). This is important because the only physiological motion permitted in the upright-MRI is lateral bending which has to be viewed in the coronal plane. Due to the design of the particular machine used in this study, only static images can be taken in the sagittal plane. So for the purpose of this study and its future applications, it may be ideal that the results are similar and the RMS errors relatively better for both techniques in the coronal plane compared to the sagittal plane.

Although the RMS error is better in the coronal plane for both techniques, they have large average RMS errors of 3.39 and 3.70 degrees, respectively. Table 14 shows a

comparison of the range of RMS error values from this study compared to those found in the literature. As stated for the translational displacements, the majority of the studies in the literature use biplanar radiography (Stokes et al. 1981 and Pearcy and Whittle 1982) or 3D Videofluoroscopy (Cholewicki et al. 1991 and Wang et al. 2008). Also, similar studies have used larger magnets and devices not applicable for in vivo use (implanted markers) to help increase the accuracy of their point selection technique (Ishii et al., 2004).

Table 14: Table comparing the ICC values obtained for the translational displacements in the present study to similar studies found in the literature.

Study	Imaging Modality	RMS Error (degrees)
Present Study	Upright-MRI	2.98-6.63
Stokes et al. (1981)	Biplanar Radiography	1.19-2.64
Pearcy and Whittle (1982)	Biplanar Radiography	0.69-1.36
Breen et al. (1988)	2D Radiography	0.30-0.84
Cholewicki et al. (1991)	3D Videofluoroscopy	0.971
Bifulco et al. (2001)	3D Videofluoroscopy	1.0
Ishii et al. (2004)	3D MRI	0.24-0.43

Additionally, the average RMS errors are larger for the trials using 2D HYCE S sequence compared to the T1 sequence for both techniques (four-point selection technique: 2D HYCE S = 5.21 degrees, T1 = 3.94 degrees; six-point selection technique: 2D HYCE S = 3.97 degrees, T1 = 3.79 degrees). The images obtained using the 2D HYCE S sequence were poorer quality than those obtained using the T1 sequence. Image quality is largely dependent on the strength of the magnet and the distinguishing features of the vertebrae. Other studies used larger magnets such as Ishii et al. (2004) as described before. Using a magnet with increased strength would have provided better

image quality and therefore more distinguishable features of the vertebrae. The images of our vertebrae had rounded corners which added difficulty in selecting the actual corner point. This was acknowledged as a possible limitation at the beginning of this study because the 2D HYCE S sequence is a dynamic sequence rather than the T1 sequence which is used for static imaging. However, according to the linear regression models for both techniques the MRI sequence is not statistically significant. Therefore, the large errors seen with the 2D HYCE S sequence may be accounted for when using the linear regression model to predict the set displacements.

Further analysis of the linear regression model provided adjusted R^2 values of 0.931 and 0.928 for the four and six-point selection technique, respectively. This suggests that 93.1% and 92.8% of the variance in the displacements of the apparatus are accounted for by the combination of the variances in the respective statistically significant variables. The four-point selection technique is similar to the translational measurements in that the measured displacement, the coronal plane, and spine 1 are significant variables. On the other hand, the six-point selection technique only had one significant variable, the measured displacement. These results suggest that the six-point selection technique is better at removing other variables that can influence the variance seen within the model.

The variance seen within the four-point selection technique comes from three variables, measured displacement, plane, and spine, but the plane and spine have a minimal influence of 0.9% of the 93.1% on the overall variance (standardized beta coefficients = -0.074 and 0.068, change in SEE = 0.06 and 0.05 degrees, respectively).

The plane may have a slight impact on the variance because the images captured in the coronal plane have enhanced quality compared to those in the sagittal plane because of the orientation. In the sagittal plane the anterior and posterior aspects of the vertebral body are more concave in comparison to the coronal plane. As stated earlier, the spine segments used were from different porcine spines and different levels of the lumbar region (L3-4 and L5-6). Although porcine vertebrae similar to human vertebrae, there are slight differences between the two. Also, the density and porosity of the bone may have been different and their functionality compromised with repeated freezing and thawing leading to decreased image quality. These factors may have decreased the accuracy of picking the correct location of the corner points of the vertebral bodies. The fact that the influence is rather minimal for the four-point selection technique and nonexistent for the six-point selection technique means that these methods have the potential to be applicable to many different segments throughout the spine.

Additional data from the regression model showed that neither point selection technique has an intercept that is significant. This means there is no bias in either method that consistently under or overestimates the rotational displacements. The slope of the measured displacement (MD) regression line is significant for both techniques (four-point selection technique = 0.637, six-point selection technique = 0.695). Ideally the slope would be 1, indicating a 1:1 relationship between the measured and actual displacements. Also, the SEE value for the four-point technique was 1.93 degrees and 2.00 degrees for the six-point selection technique. This means that a measurement of rotational movement

is within ±3.86 degrees for the four-point selection technique and ±4.00 degrees for the six-point selection technique with 95% certainty.

In regards to the repeatability of measuring rotational displacements with our point selection techniques, the ICC values for both intraobserver and interobserver shown in Table 15 show very strong agreement. The ICC(2,2) values are slightly weaker compared to the ICC(2,1) values but still show moderate agreement. Besides the ICC(2,2) values for the sagittal orientation, all the values are greater than 0.927 with many of them showing an almost near perfect agreement of 1. There does not appear to be a difference between the ICC(2,1) values for the four and six-point selection technique. This indicates that both techniques are acceptable as highly repeatable methods of measuring rotational displacements. The linear regression analysis supports this claim because the day variable was found to not be statistically significant. Table 12 shows the ICC values from this study compared to other values reported in the literature. Our values are comparable and even better than some studies using similar manual measuring techniques. Similarly, our values are comparable to studies using computer-assisted methods. This demonstrates that our method is highly repeatable for one person or multiple people performing the point selections on different days.

Table 15: Table comparing the ICC values for the rotational displacements obtained in the present study to similar studies found in the literature.

ICC Values				
Study	**Manual or Computer-Assisted**	**Model**	**Intraobserver ICC**	**Interobserver ICC**
Present Study	Manual	2	0.959-0.998	0.819-0.930
Teyhen et al. (2005)	Manual	2	0.966-0.993	0.637-0.944
Fritz et al. (2005)	Manual	2	0.84-0.99	-
Pearson et al. (2011)	Manual	3	0.083-0.866	-0.122-0.780
Pearson et al. (2011)	Computer-Assisted	3	0.741-0.990	0.343-0.962
Yeager et al. (2014)	Manual	3	0.625	0.551
Yeager et al. (2014)	Computer-Assisted	3	0.983	0.958

Based on these results, it can be concluded that by using an increased number of points to measure rotational displacements it eliminates all outside variables but seems to decrease the accuracy of the measurements. Also, the repeatability of both techniques is strong. Our measurement technique may not be the most appropriate way of achieving accurate rotational measurements. There are several similar studies that have performed techniques to help improve the accuracy of their study. Some have helped with the point selection technique such as Pearcy and Whittle (1982) which selected nine points on each vertebra. Similarly, Bifulco et al. (2001) created a template based on the points selected on the first image for the subsequent images. Others have used different methods involving a bisetrix for magnified images and to reduce the variability seen between different vertebral anatomy such as Frobin et al., (1996). Lastly, Teyhen et al. (2005) used a series of image enhancement techniques to remove noise in each image and to

enhance the landmarks of the vertebral bodies. Our next step is exploring these and other potential improvements to this method to either increase the accuracy of selecting the corner points or altering the method in a way that is better suited for the images we are able to capture.

REFERENCES

Allbrook, D., 1957. Movements of the Lumbar Spinal Column. The Journal of Bone and Joint Surgery 39B (2), 339-345.

American Cancer Society. Cancer Facts & Figures 2016. Atlanta: American Cancer Society; 2016.

Begg, C., Falconer, M., 1949. Plain radiography in intraspinal protrusion of lumbar intervertebral disks: a correlation with operative findings. The British Journal of Surgergy 26 (143), 225-239.

Bevel, P. (2010). The Fourier Transform. Retrieved from http://www.thefouriertransform.com/#introduction

Bifulco, P., Cesarelli, M., Allen, R., Sansone, M., Bracale, M., 2001. Automatic recognition of vertebral landmarks in fluoroscopic sequences for analysis of intervertebral kinematics. Medical & Biological Engineering and Computing 39, 65-75.

Breen, A., Allen, R., Morris, A., 1988. An image processing method for spine kinematics-preliminary studies. Clinical Biomechanics 3, 5-10.

Breen, A., Allen,. R., Morris, A., 1989. Spine kinematics: a digital videofluoroscopic technique. Journal of Biomedical Engineering 11, 224-228.

Burk, Brett, 2010. Radiation Risk in Perspective. Position Statement of the Health Physics Society, 1-3.

Busscher, I., Ploegmakers, J., Verkerke, G., Veldhuizen, A., 2010. Comparative anatomical dimensions of the complete human and porcine spine. European Spine Journal 19 (7), 1104-1114.

Cholewicki, J., McGill, S., Wells, R., Vernon, H., 1991. Method for measuring vertebral kinematics from videofluoroscopy. Clinical Biomechanics 6, 73-78.

Cochard, L. R., Goodhartz, L. A., Harmath, C. B., Major, N. M., Mukundan, S. (2012). Netter's Introduction to Imaging. Elsevier.

Dalton, E. (2008, August). Don't Get Married, Part 2. *Massage Today, 8 (8).* Retrieved from http://www.massagetoday.com/mpacms/mt/article.php?id=13852

Dimnet, J., Fischer, L., Gonon, G., Carret, J., 1978. Radiographic studies of lateral flexion in the lumbar spine. Journal of Biomechanics 11, 143-150.

Dvorak, J., Panjabi, M., Chang, D., Theiler, R., Grob, D., 1991. Functional Radiographic Diagnosis of the Lumbar Spine: Flexion-Extension and Lateral Bending. Spine 16 (5), 562-571.

Fiebert, I. M., Spyropoulos, T., Peterman, D., 1993. Thoracic segmental flexion during cervical forward bending. Journal of Back and Musculoskeletal Rehabilitation 3 (4), 80-85.

Fritz, J., Piva, S., Childs, J., 2005. Accuracy of the clinical examination to predict radiographic instability of the lumbar spine. European Spine Journal 14, 743-750.

Frobin, W., Brinckmann, P., Leivseth, G., Biggemann, M., Reikeras, O., 1996. Precision measurement of segmental motion from flexion-extension radiographs of the lumbar spine. Clinical Biomechanics 11 (8), 457-465.

Froning, E., Frohman, B., 1968. Motion of the Lumbosacral Spine After Laminectomy and Spine Fusion. The Journal of Bone and Joint Surgery 50, 897-918.

Fujii, R., Sakaura, H., Mukai, Y., Hosono, N., Ishii, T., Iwasaki, M., Yoshikawa, H., Sugamoto, K., 2007. Kinematics of the lumbar spine in trunk rotation: in vivo three-dimensional analysis using magnetic resonance imaging. European Spine Journal 16, 1867-1874.

Gould, T. A., Edmonds, M. (2008). How MRI Works. Retrieved from http://science.howstuffworks.com/mri3.htm

Ha, K., Son, J., Im, J., Oh, I., 2013. Risk factors for adjacent segment degeneration after surgical correction of degenerative lumbar scoliosis. Indian Journal of Orthopaedics 47 (4), 346-351.

Hanley, Jr, E., Matteri, R., Frymoyer, J., 1976. Accurate Roentgenographic Determination of Lumbar Flexion-Extension. Clinical Orthopaedics and Related Research 115, 145-148.

Harvey, S., Hukins, D., 1998. Measurement of lumbar spinal flexion-extension kinematics from lateral radiographs: simulation of the effects of out-of-plane movement and errors in reference point placement. Medical Engineering & Physics 20, 403-409.

Hayes, M., Howard, T., Gruel, C., Kopta, J., 1989. Roentgenographic Evaluation of Lumbar Spine Flexion-Extension in Asymptomatic Individuals. Spine 14 (3), 327-331.

IBM Corp. Released 2012. IBM SPSS Statistics for Windows, Version 21.0. Armonk, NY: IBM Corp.

Ishii, T., Mukai, Y., Hosono, N., Sakaura, H., Nakajima, Y., Sato, Y., Sugamoto, K., Yoshikawa, H., 2004. Kinematics of the Upper Cervical Spine in Rotation. Spine 29 (7), E139-E144.

Kanayama, M., Abumi, K., Kaneda, K., Tadano, S., Ukai, T., 1996. Phase Lag of the Intersegmental Motion in Flexion-Extension of the Lumbar and Lumbosacral Spine: An In Vivo Study. Spine 21 (12), 1416-1422.

Kozanek, M., Wang, S., Passias, P., Xia, Q., Li, Ga., Bono, C. M., Wood, K. B., Li, Gu., 2009. Range of Motion and Orientation of the Lumbar Facet Joints In Vivo. Spine 34 (19), E689-E696.

Lee, S., Wong, K., Chan, M., Yeung, H., Chiu, J., Leong, J., 2002. Development and Validation of a New Technique for Assessing Lumbar Spine Motion. Spine 27 (8), E215-E220.

Lemonick, D., 2009. "Oh, My Aching Back!" An Evidence-Based Review of One of Mankind's Oldest Afflictions. American Journal of Clinical Medicine 6 (4), 5-13.

Li, G., Wang, S., Passias, P., Xia, Q., Li, G., Wood, K., 2009. Segmental in vivo vertebral motion during functional human lumbar spine activities. European Spine Journal 18, 1013-1021.

Mahaudens, P., Thonnard, J., Detrembleur, C., 2005. Influence of structural pelvic disorders during standing and walking in adolescents with idiopathic scoliosis. The Spine Journal 5, 427-433.

McGregor, A., Anderton, L., Gedroyc, W., Johnson, J., Hughes, S., 2001. Assessment of Spinal Kinematics Using Open Interventional Magnetic Resonance Imaging. Clinical Orthopaedics and Related Research 392, 341-348.

Modic, M. T., Masaryk, T. J., Ross, J. S. (1989). Magnetic Resonance Imaging of the Spine. Chicago: Year Book Medical Publishers, Inc.

Moreside, J., Barbado, D., Juan-Recio, C., Vera-Garcia, F., 2013. Active hip and spine ROM differs when comparing unconstrained motion with voluntary segmental constraint. Manual Therapy 18, 557-561.

Muggleton, J., Allen, R., 1998. Insights into the measurement of vertebral translation in the sagittal plane. Medical Engineering & Physics 20, 21-32.

Muggleton, J., Kondracki, M., Allen, R., 2000. Spinal Fusion for Lumbar Instability: Does It Have a Scientific Basis? Journal of Spinal Disorders 13 (3), 200-204.

Nguyen, H. S., Doan, N., Shabani, S., Baisden, J., Wolfla, C., Paskoff, G., Shender, B., Stemper, B., 2016. Upright magnetic resonance imaging of the lumbar spine: Back pain and radiculopathy. Journal of Craniovertebral Junction and Spine 7 (7), 31-37.

Okawa, A., Shinomiya, K., Komori, H., Muneta, T., Arai, Y., Nakai, O., 1998. Dynamic Motion Study of the Whole Lumbar Spine by Videofluoroscopy. Spine 23 (16), 1743-1749.

Page, W., Monteith, W., 1992. Bone Movement Analysis From Computer Processing of X-ray Cinematic Video Images. International Conference on Image Processing and its Applications 354, 381-384.

Panjabi, M., Chang, D., Dvorak, J., 1992. An Analysis of Errors in Kinematic Parameters Associated with in Vivo Functional Radiographs. Spine 17 (2), 200-205.

Passias, P.G., Wang, S., Kozanek, M., Xia, Q., Li, W., Grottkau, B., Wood, K.B., Li, G., 2011. Segmental Lumbar Rotation in Patients with Discogenic Low Back Pain During Functional Weight-Bearing Activities. The Journal of Bone and Joint Surgery 93 (1), 29-37.

Pearcy, M., Hindle, R., 1989. New method for the non-invasive three-dimensional measurement of human back movement. Clinical Biomechanics 4, 73-79.

Pearcy, M., Portek, I., Shepherd, J., 1984. Three-Dimensional X-ray Analysis of Normal Movement in the Lumbar Spine. Spine 9 (3), 294-297.

Pearcy, M., Portek, I., Shepher, J., 1985. The Effect of Low-Back Pain on Lumbar Spinal Movements Measured by Three-Dimensional X-Ray Analysis. Spine 10 (2), 150-153.

Pearcy, M., Whittle, M., 1982. Movements of the lumbar spine measured by three-dimensional x-ray analysis. Journal of Biomedical Engineering 4, 107-112.

Pearson, A., Spratt, K., Genuario, J., McGough W., Kosman, K., Lurie, J., Sengupta, D., 2011. Precision of Lumbar Intervertebral Measurements: Does a Computer-Assisted Technique Improve Reliability? Spine 36 (7), 572-580.

Pope, M., Frymoyer, J., Krag, M., 1992. Diagnosing Instability. Clinical Orthopaedics and Related Research 279, 60-67.

R Core Team, 2013. R: A language and environment for statistical computing. R Foundation for Statistical Computing, Vienna, Austria. ISBN 3-900051-07-0, URL http://www.R-project.org/

Rodriguez-Soto, A. E., Jaworski, R., Jensen, A., Niederberger, B., Hargens, A. R., Frank, L. R., Kelly, K. R., Ward, S. R., 2013. Effect of Load Carriage on Lumbar Spine Kinematics. Spine 38 (13), E783-E791.

Shaffer, W., Spratt, K., Weinstein, J., Lehmann, T., Goel, V., 1990. The Consistency and Accuracy of Roentgenograms for Measuring Sagittal Translation in the Lumbar Vertebral Motion Segment: An Experimental Model. Spine 15 (8), 741-750.

Shin, J., Wang, S., Yao, Q., Wood, K., Li, G., 2013. Investigation of coupled bending of the lumbar spine during dynamic axial rotation of the body. European Spine Journal 22, 2671-2677.

Shrout, P., Fleiss, J., 1979. Intraclass Correlations: Uses in Assessing Rater Reliability. Psychological Bulletin 86 (2), 420-428.

Shymon, S., Hargens, A. R., Minkoff, L. A., Chang, D. G., 2014. Body posture and backpack loading: an upright magnetic resonance imaging study of the adult lumbar spine. European Spine Journal 23, 1407-1413.

Splendiani, A., Perri, M., Grattacaso, G., Di Tunno, V., Marsecano, C., Panebianco, L., Gennarelli, A., Felli, V., Varrassi, M., Barile, A., Di Cesare, E., Masciocchi, C., Gallucci, M., 2016. Magnetic resonance imaging (MRI) of the lumbar spine with dedicated G-scan machine in the upright position: a retrospective study and our experience in 10 years with 4305 patients. La Radiologia Medica 121 (1), 38-44.

Stokes, I., Frymoyer, J., 1987. Segmental Motion and Instability. Spine 12 (7), 688-691.

Stokes, I., Wilder, D., Frymoyer, J., Pope, M., 1981. Assessment of Patients with Low-Back Pain by Biplanar Radiographic Measurement of Intervertebral Motion. Spine 6 (3), 233-240.

Tanz, S., 1953. Motion of the lumbar spine. The American Journal of Roentgenology, Radian Therapy and Nuclear Medicine 69 (3), 399-412.

Tarantino, U., Fanucci, E., Iundusi, R., Celi, M., Altobelli, S., Gasbarra, E., Simonetti, G., Manenti, G., 2013. Lumbar spine MRI in upright position for diagnosing acute and chronic low back pain: statistical analysis of morphological changes. Journal of Orthopaedics and Traumatology 14, 15-22.

Taylor, J., Twomey, L., 1980. Sagittal and horizontal plane movement of the human lumbar vertebral column in cadavers and in the living. Rheumatology and Rehabilitation 19, 223-232.

Teyhen, D., Flynn, T., Bovik, A., Abraham, L., 2005. A New Technique for Digital Fluoroscopic Video Assessment of Sagittal Plane Lumbar Spine Motion. Spine 30 (14), E406-E413.

Teyhen, D., Flynn, T., Childs, J., Abraham, L., 2007. Arthrokinematics in a Subgroup of Patients Likely to Benefit From a Lumbar Stabilization Exercise Program. Physical Therapy 87 (2), 313-325.

Thurston, A., Harris, J., 1983. Normal Kinematics of the Lumbar Spine and Pelvis. Spine 8 (2), 199-205.

Van Mameren, H., Drukker, J., Sanches, H., Beursgens, J., 1990. Cervical Spine Motion in the Sagittal Plane (I) Range of Motion of Actually Performed Movements, an X-ray Cinematographic Study. European Journal of Morphology 28 (1), 47-68.

Wang, S., Passias, P., Li, Ga., Li, Gu., Wood, K., 2008. Measurement of Vertebral Kinematics Using Noninvasive Image Matching Method-Validation and Application. Spine 33 (11), E355-E361.

White, III, A., Panjabi, M., 1978. The Basic Kinematics of the Human Spine: A Review of Past and Current Knowledge. Spine 3 (1), 12-20.

White, III, A., Panjabi, M. (1990). Clinical Biomechanics of the Spine: Second Edition. Philadelphia: J. B. Lippincott Company.

Wiles, P., 1935. Movements of the Lumbar Vertebrae during Flexion and Extension. Proceedings of the Royal Society of Medicine, 647-651.

Winter, B., 2013. Linear models and linear mixed effects models in R with linguistic applications. 1-42.

Xia, Q., Wang, S., Kozanek, M., Passias, P., Wood, K., Li, G., 2010. In-vivo motion characteristics of lumbar vertebrae in sagittal and transverse planes. Journal of Biomechanics 43, 1905-1909.

Yeager, M., Cook, D., Cheng, B., 2014. Reliability of computer-assisted lumbar intervertebral measurements using a novel vertebral motion analysis system. The Spine Journal 14, 274-281.

APPENDIX A: TRANSLATIONS

```
Call:
lm(formula = SD ~ MD + CorPlane + HySeq + Day1 + Spine1, data = tdata)

Residuals:
     Min       1Q   Median       3Q      Max
-1.54014 -0.37201 -0.01788  0.42361  1.40554

Coefficients:
            Estimate Std. Error t value Pr(>|t|)
(Intercept)  -0.6004     0.1213  -4.950 2.41e-06 ***
MD            1.1282     0.0183  61.661  < 2e-16 ***
CorPlane      0.4440     0.1085   4.092 7.70e-05 ***
HySeq         0.1003     0.1084   0.926  0.35648
Day1         -0.0292     0.1084  -0.269  0.78807
Spine1        0.3575     0.1085   3.294  0.00129 **
---
Signif. codes:  0 '***' 0.001 '**' 0.01 '*' 0.05 '.' 0.1 ' ' 1

Residual standard error: 0.6131 on 122 degrees of freedom
Multiple R-squared:  0.9689,    Adjusted R-squared:  0.9676
F-statistic: 760.7 on 5 and 122 DF,  p-value: < 2.2e-16
```

Figure 31: Initial output in R of the linear regression model showing significant variables, standard errors, and R^2 values.

```
Call:
lm(formula = SD ~ MD + CorPlane + Spine1, data = tdata)

Residuals:
     Min       1Q   Median       3Q      Max
-1.47374 -0.43229 -0.00113  0.42675  1.37089

Coefficients:
            Estimate Std. Error t value Pr(>|t|)
(Intercept) -0.56480    0.09359  -6.035 1.71e-08 ***
MD           1.12796    0.01822  61.921  < 2e-16 ***
CorPlane     0.44396    0.10804   4.109 7.16e-05 ***
Spine1       0.35743    0.10807   3.307  0.00123 **
---
Signif. codes:  0 '***' 0.001 '**' 0.01 '*' 0.05 '.' 0.1 ' ' 1

Residual standard error: 0.6104 on 124 degrees of freedom
Multiple R-squared:  0.9687,    Adjusted R-squared:  0.9679
F-statistic:  1279 on 3 and 124 DF,  p-value: < 2.2e-16
```

Figure 32: Output in R of the linear regression model with non-statistically significant variables removed from the model. It shows the significant variables, standard errors, and R^2 values.

APPENDIX B: ROTATIONS

```
Call:
lm(formula = SD ~ MD + CorPlane + HySeq + Day1 + Spine1, data = rdata)

Residuals:
    Min      1Q  Median      3Q     Max
-5.9287 -1.4253 -0.1406  1.4240  5.3943

Coefficients:
            Estimate Std. Error t value Pr(>|t|)
(Intercept)  0.11491    0.40385   0.285  0.77648
MD           0.63800    0.01669  38.235  < 2e-16 ***
CorPlane    -1.07771    0.35877  -3.004  0.00323 **
HySeq        0.52041    0.33988   1.531  0.12833
Day1        -0.17419    0.33964  -0.513  0.60898
Spine1       0.99127    0.34060   2.910  0.00429 **
---
Signif. codes:  0 '***' 0.001 '**' 0.01 '*' 0.05 '.' 0.1 ' ' 1

Residual standard error: 1.921 on 122 degrees of freedom
Multiple R-squared:  0.9339,    Adjusted R-squared:  0.9312
F-statistic: 344.8 on 5 and 122 DF,  p-value: < 2.2e-16
```

Figure 33: Initial output in R of the linear regression model for the four-point selection technique showing significant variables, standard errors, and R^2 values.

```
Call:
lm(formula = SD ~ MD + CorPlane + HySeq + Day1 + Spine1, data = rdata)

Residuals:
    Min      1Q  Median      3Q     Max
-4.5061 -1.3566 -0.1741  1.5685  4.1064

Coefficients:
            Estimate Std. Error t value Pr(>|t|)
(Intercept) -0.27085    0.41706  -0.649   0.5173
MD           0.69707    0.01870  37.286   <2e-16 ***
CorPlane    -0.04943    0.37706  -0.131   0.8959
HySeq        0.34828    0.34770   1.002   0.3185
Day1        -0.62741    0.34798  -1.803   0.0739 .
Spine1       0.67335    0.34804   1.935   0.0553 .
---
Signif. codes:  0 '***' 0.001 '**' 0.01 '*' 0.05 '.' 0.1 ' ' 1

Residual standard error: 1.966 on 122 degrees of freedom
Multiple R-squared:  0.9308,    Adjusted R-squared:  0.9279
F-statistic: 328.1 on 5 and 122 DF,  p-value: < 2.2e-16
```

Figure 34: Initial output in R of the linear regression model for the six-point selection technique showing significant variables, standard errors, and R^2 values.

```
Call:
lm(formula = SD ~ MD + CorPlane + Spine1, data = rdata)

Residuals:
    Min      1Q  Median      3Q     Max
-5.5667 -1.4361 -0.1215  1.4216  5.7147

Coefficients:
            Estimate Std. Error t value Pr(>|t|)
(Intercept)  0.29709    0.32354   0.918  0.36028
MD           0.63687    0.01671  38.108  < 2e-16 ***
CorPlane    -1.08559    0.35961  -3.019  0.00308 **
Spine1       0.98950    0.34143   2.898  0.00444 **
---
Signif. codes:  0 '***' 0.001 '**' 0.01 '*' 0.05 '.' 0.1 ' ' 1

Residual standard error: 1.926 on 124 degrees of freedom
Multiple R-squared:  0.9325,    Adjusted R-squared:  0.9309
F-statistic: 571.1 on 3 and 124 DF,  p-value: < 2.2e-16
```

Figure 35: Output in R of the linear regression model for the four-point selection technique with non-statistically significant variables removed from the model. It shows the significant variables, standard errors, and R^2 values.

```
Call:
lm(formula = SD ~ MD, data = rdata)

Residuals:
    Min      1Q  Median      3Q     Max
-4.4086 -1.4465 -0.1488  1.3809  4.4933

Coefficients:
            Estimate Std. Error t value Pr(>|t|)
(Intercept) -0.08887    0.18926   -0.47    0.639
MD           0.69462    0.01746   39.78   <2e-16 ***
---
Signif. codes:  0 '***' 0.001 '**' 0.01 '*' 0.05 '.' 0.1 ' ' 1

Residual standard error: 1.997 on 126 degrees of freedom
Multiple R-squared:  0.9262,    Adjusted R-squared:  0.9257
F-statistic:  1582 on 1 and 126 DF,  p-value: < 2.2e-16
```

Figure 36: Output in R of the linear regression model for the six-point selection technique with non-statistically significant variables removed from the model. It shows the significant variables, standard errors, and R^2 values.

Thesis and Dissertation Services